

Dual Filter: A Transformer-like Inference Architecture for Hidden Markov Models

Heng-Sheng Chang

*Coordinated Science Laboratory
University of Illinois Urbana-Champaign
Urbana, IL 61801, USA*

HSCHANG@ILLINOIS.EDU

Prashant G. Mehta

*Coordinated Science Laboratory
University of Illinois Urbana-Champaign
Urbana, IL 61801, USA*

MEHTAPG@ILLINOIS.EDU

Abstract

This paper presents a mathematical framework for causal nonlinear prediction in settings where observations are generated from an underlying hidden Markov model (HMM). Both the problem formulation and the proposed solution are motivated by the decoder-only transformer architecture, in which a finite sequence of observations (tokens) is mapped to the conditional probability of the next token. Our objective is not to construct a mathematical model of a transformer. Rather, our interest lies in deriving, from first principles, transformer-like architectures that solve the prediction problem for which the transformer is designed. The proposed framework is based on an original optimal control approach, where the prediction objective (MMSE) is reformulated as an optimal control problem. An analysis of the optimal control problem is presented leading to a fixed-point equation on the space of probability measures. To solve the fixed-point equation, we introduce the dual filter, an iterative algorithm that closely parallels the architecture of decoder-only transformers. These parallels are discussed in detail along with the relationship to prior work on mathematical modeling of transformers as transport on the space of probability measures. Numerical experiments are provided to illustrate the performance of the algorithm using parameter values typical of research-scale transformer models.

Keywords: Nonlinear predictor, transformer, stochastic control, optimal control, hidden Markov model.

1 Introduction

Let $\mathbb{O} = \{0, 1, 2, \dots, m\}$ denote a finite set called the vocabulary. An element of \mathbb{O} is referred to as a token. A sequence of T tokens is an \mathbb{O}^T -valued random vector, denoted by $\{Z_1, Z_2, \dots, Z_T\}$. A decoder-only transformer is an algorithm to compute the conditional probability of the next token (see Phuong and Hutter (2022)):

$$P(Z_{T+1} = z \mid Z_1, Z_2, \dots, Z_T), \quad z \in \mathbb{O}.$$

During inference with a well-trained transformer, the conditional probability is often sparse—that is, only a small subset of tokens has non-negligible probability. This sparsity is useful for efficient sampling in generative AI applications (Wolfram, 2023).

There are two distinguishing features of the decoder-only transformer architecture:

1. Even though only the conditional probability at the terminal time $t = T$ is of interest, conditional probabilities are also computed for intermediate times,

$$P(Z_{t+1} = z \mid Z_1, Z_2, \dots, Z_t), \quad z \in \mathbb{O}, \quad t = 1, 2, \dots, T.$$

2. In all cases, the conditional probability of the next token is expressed as a causal, nonlinear function of the past tokens, implemented through a procedure known as causal masking. In this paper, we refer to such a function as a nonlinear predictor (a formal definition is given after the model has been introduced).

The second item is in contrast to a recurrent neural network (RNN) architecture, where a hidden state is stored and recursively updated (Graves, 2013; Dai et al., 2019).

A transformer architecture is reminiscent of the classical Wiener filter. Recall that a Wiener filter computes the conditional expectation of a Gaussian process, also denoted (with slight abuse of notation) as $[Z_1, Z_2, \dots, Z_T]$, in the following causal form:

$$E(Z_{T+1} \mid Z_1, Z_2, \dots, Z_T) = (\text{constant}) + \sum_{t=1}^T u_t^T Z_t.$$

The right-hand side is an example of a linear predictor where $u := \{u_t \in \mathbb{R}^{m \times m} : 1 \leq t \leq T\}$ are deterministic weights, to be designed or learned. The Wiener filtering theory is concerned with the synthesis of the optimal weights that yield the conditional expectation (Kailath et al., 2000, Ch. 7).

The objective of this paper is to develop both theory and algorithms for a nonlinear predictor, that computes the conditional probability of the next token, for a large but finite vocabulary. Our focus is exclusively on inference, not on learning. To this end, we adopt a model-based approach based on a hidden Markov model (HMM), where the observed tokens are generated from an underlying hidden stochastic process. This process evolves as a Markov chain, taking values in a finite state space of dimension d . We begin by describing the model and then introducing the problem.

1.1 Math Preliminaries: Hidden Markov model and the nonlinear filter

Throughout this paper, we consider discrete-time stochastic processes on a finite time-horizon $\mathbb{T} = \{0, 1, 2, \dots, T\}$ with $T < \infty$. Fix the probability space $(\Omega, \mathcal{F}_T, P)$ along with the filtration $\{\mathcal{F}_t : t \in \mathbb{T}\}$ with respect to which all the stochastic processes are adapted. A hidden Markov model (HMM) is specified by a pair of stochastic processes (X, Z) defined as follows (see Elliott et al. (2008); Cappé et al. (2006)):

1. The state-space $\mathbb{S} = \{1, 2, \dots, d\}$ is finite.
2. The observation-space $\mathbb{O} = \{0, 1, 2, \dots, m\}$ is finite of cardinality $|\mathbb{O}| = m + 1$. (With $m = 1$, there are only two observations $\mathbb{O} = \{0, 1\}$. Such an HMM is referred to as the binary-valued HMM.)
3. The state process $X = \{X_t : t \in \mathbb{T}\}$ is a Markov chain taking values in the state-space \mathbb{S} . Its time-evolution is modeled as

$$P(X_0 = x) = \mu(x), \quad x \in \mathbb{S}.$$

$$P(X_{t+1} = x' \mid X_t = x) = A(x, x'), \quad x, x' \in \mathbb{S}, \quad t = 0, 1, 2, \dots, T - 1.$$

The matrix A is row stochastic, meaning that for each $x \in \mathbb{S}$, $A(x, \cdot)$ is a probability vector.

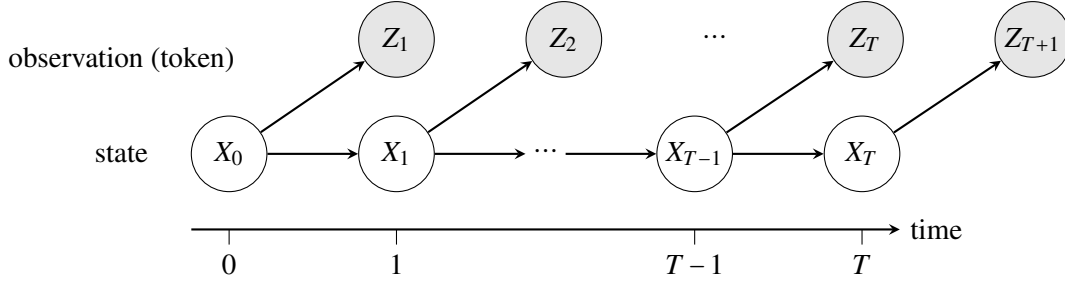


Figure 1: Graphical model for the HMM.

4. The observation process $Z = \{Z_1, Z_2, \dots, Z_T\}$ takes values in \mathbb{O} . Its model is given by

$$P(Z_{t+1} = z | X_t = x) = C(x, z), \quad z \in \mathbb{O}, x \in \mathbb{S}, \quad t = 0, 1, 2, \dots, T-1.$$

The matrix C is row stochastic, meaning that for each $x \in \mathbb{S}$, $C(x, \cdot)$ is a probability vector.

The model is succinctly denoted by $(X, Z) = \text{HMM}(\mu, A, C)$.

For the purposes of mathematical analysis, the filtrations are introduced as follows:

$$\begin{aligned} \mathcal{F}_t &:= \sigma(X_0, Z_1, X_1, \dots, Z_t, X_t), \quad t \in \mathbb{T}, \\ \mathcal{Z}_t &:= \sigma(Z_1, Z_2, \dots, Z_t), \quad t = 1, 2, \dots, T, \end{aligned}$$

with $\mathcal{Z}_0 := \{\phi, \Omega\}$. $\mathcal{F} = \{\mathcal{F}_t : t \in \mathbb{T}\}$ is referred to as the canonical filtration with respect to which all processes are adapted. The graphical model for the HMM is depicted in Fig. 1.

Notation: The spaces of signed measures on \mathbb{S} and \mathbb{O} are denoted by $\mathcal{M}(\mathbb{S})$ and $\mathcal{M}(\mathbb{O})$, respectively, and the set of probability measures $\mathcal{P}(\mathbb{S}) \subset \mathcal{M}(\mathbb{S})$ and $\mathcal{P}(\mathbb{O}) \subset \mathcal{M}(\mathbb{O})$. The space of signed-measures and functions on \mathbb{S} are both identified with \mathbb{R}^d : a real-valued function f (resp., a measure μ) is identified with a column vector in \mathbb{R}^d where the x^{th} element of the vector represents $f(x)$ (resp., $\mu(x)$), for $x \in \mathbb{S}$, and $\mu(f) := \mu^T f = \sum_x \mu(x) f(x)$. Lower case symbol, e.g., f , is used to denote a deterministic function while an upper case symbol, e.g., F , is used to denote a random function. For such a function, the notation $F \in \mathcal{Z}_t$ means $F(x)$ is \mathcal{Z}_t -measurable for each $x \in \mathbb{S}$. A product of two functions f and g is denoted by fg ($(fg)(x) = f(x)g(x)$ for $x \in \mathbb{S}$), and $f^2 = ff$. The unity function is denoted by 1 (e.g., as a function on \mathbb{S} , $1(x) = 1$ for all $x \in \mathbb{S}$). For a vector $f \in \mathbb{R}^d$, $\text{diag}(f)$ is $d \times d$ diagonal matrix with entries given by the components of f . We follow the convention $\frac{0}{0} = 0$.

Nonlinear filter: The objective of nonlinear (or stochastic) filtering is to compute the conditional measure, also called the posterior. It is defined as a conditional expectation,

$$\pi_t(f) := \mathbb{E}(f(X_t) | \mathcal{Z}_t), \quad f \in \mathbb{R}^d, \quad t \in \mathbb{T}.$$

A recursive formula for the same is given by

$$\pi_{t+1}(f) = \frac{\pi_t(\text{diag}(C(:, Z_{t+1}))Af)}{\pi_t(\text{diag}(C(:, Z_{t+1}))1)}, \quad t = 0, 1, 2, \dots, T-1, \quad \pi_0 = \mu.$$

The formula is referred to as the nonlinear filter, also called the forward algorithm. The convention $\frac{0}{0} = 0$ is used to handle the case where the denominator is zero (note in which case the numerator must also be zero).

For the prediction problem, the conditional probability is denoted by

$$p_t(z) := \mathbb{P}(Z_{t+1} = z \mid Z_1, Z_2, \dots, Z_t), \quad t \in \mathbb{T},$$

where note $p_0(z) = \mathbb{P}(Z_1 = z)$. It is computed from the nonlinear filter as

$$p_t = \pi_t(C), \quad \text{that is,} \quad p_t(z) = \sum_{x \in \mathbb{S}} \pi_t(x) C(x, z), \quad z \in \mathbb{O}, \quad t \in \mathbb{T}.$$

We denote

$$\pi := \{\pi_t : t \in \mathbb{T}\}, \quad p := \{p_t : t \in \mathbb{T}\}.$$

The stochastic processes π and p take values in $\mathcal{P}(\mathbb{S})$ and $\mathcal{P}(\mathbb{O})$, respectively.

1.2 Problem statement (theory)

Define a vector-valued mapping $e : \mathbb{O} \rightarrow \mathbb{R}^m$ as follows:

$$e(1) = \begin{bmatrix} 1 \\ 0 \\ \vdots \\ 0 \end{bmatrix}_{m \times 1}, \quad e(2) = \begin{bmatrix} 0 \\ 1 \\ \vdots \\ 0 \end{bmatrix}_{m \times 1}, \quad \dots \quad e(m) = \begin{bmatrix} 0 \\ 0 \\ \vdots \\ 1 \end{bmatrix}_{m \times 1}, \quad e(0) = -e(1) - e(2) - \dots - e(m) = \begin{bmatrix} -1 \\ -1 \\ \vdots \\ -1 \end{bmatrix}_{m \times 1}.$$

(Recall here that the cardinality $|\mathbb{O}| = m + 1$.)

Example 1 (m=1) Consider the HMM with binary-valued observations where recall $\mathbb{O} = \{0, 1\}$. For this model,

$$e(1) = 1, \quad e(0) = -1.$$

Our theory goal is to derive the following representation for the conditional measure:

$$\pi_T(F) = (\text{constant}) - \sum_{t=1}^T U_{t-1}^T e(Z_t), \quad \text{P-a.s.,} \quad F \in \mathcal{Z}_T, \quad (1)$$

where $U = \{U_0, U_1, \dots, U_{T-1}\}$ is a \mathcal{Z} -adapted stochastic process taking values in \mathbb{R}^m . The representation in (1) is referred to as a *nonlinear predictor*.

The following remarks draw an analogy, from an input-output perspective, to the Wiener filter and the transformer.

Remark 1 (Linear vs nonlinear predictors) Compare (1) with the representation for the linear predictor. While the weights u in a linear predictor are deterministic, the weights in a nonlinear predictor are random—i.e., U_t is allowed to depend upon past observations $\{Z_1, Z_2, \dots, Z_t\}$ for each $0 \leq t \leq T - 1$. This dependence is what makes the predictor nonlinear.

Remark 2 (Input (tokens)) The mapping $e : \mathbb{O} \rightarrow \mathbb{R}^m$ is reminiscent of the “one-hot encoding” of tokens, and may be regarded as such. It differs slightly, however, because here the vocabulary size is $|\mathbb{O}| = m + 1$. The form of $e(\cdot)$ is chosen for well-posedness of the representation in (1) (Prop. 6).

Remark 3 (Output (prediction at time T)) Taking the function F as $F(x) = C(x, z)$ yields a nonlinear predictor for $p_T(z)$, for $z \in \mathbb{O}$. The key point is that the prediction is computed using the representation (1).

Remark 4 (Predictions for intermediate times) Because U is \mathcal{Z} -adapted, the partial sum of the expression on the right-hand side of (1),

$$S_t = (\text{constant}) - \sum_{s=1}^t U_{s-1}^T e(Z_s), \quad \text{at any intermediate time } t = 1, 2, \dots, T,$$

is \mathcal{Z}_t -measurable (i.e., depends only on the observation sequence $\{Z_1, Z_2, \dots, Z_t\}$ up to time t). In this paper, the partial sum is related to the conditional measure $\pi_t(\cdot)$, which is helpful to establish a connection to the decoder-only transformer where causal predictions are computed for $1 \leq t \leq T$.

1.3 Contributions of this paper

The main contributions of our paper are as follows:

1. We begin by proving a well-posedness (existence) result (for U) such that the representation in (1) holds (Prop. 6). The remainder of the paper is concerned with the design and numerical approximation of this U . The two objectives inform the split of the paper—theory for design in Sec. 2 and algorithms for approximation in Sec. 3.
2. The theoretical contribution is an explicit formula for U (Thm. 11). The formula is derived using an original optimal control approach, referred to as the *duality theory* for HMMs. A precise statement of the duality—between nonlinear filtering and optimal control—is given in the form of a duality principle (Thm. 9). Based on this, U is shown to admit an interpretation as an optimal control input (Prop. 10).
3. The formula for U yields a fixed-point representation of the conditional measure π . This in turn suggests a natural definition for a (transformer-like) layer transformation $\mathcal{N}^{(\text{dfitr})}$ on the space of probability measures (Fig. 2 in Sec. 4.3).
4. The algorithmic contribution is the dual filter algorithm, which approximates π by iterative application of $\mathcal{N}^{(\text{dfitr})}$ (Sec. 3.1). The algorithm has complexity $O(d^2T)$, which is independent of the vocabulary size m and therefore scales efficiently to large vocabularies.
5. The paper closes with numerics. While we do not include learning, the dimension of HMM is chosen to mimic the so-called ‘GPU parameters’ used in certain models of transformers ($d = 384$, $m = 65$, and $T = 256$) (Karpathy, 2022).

The paper makes original contributions to *both* nonlinear filtering and control theory:

1. The representation (1) for causal nonlinear predictor is new.
2. Duality theory for HMMs is an original contribution of this paper, and resolves a longstanding open problem in control theory. This is explained as part of Sec. 2.5.

In order to relate our work to transformers, a self-contained description of the decoder-only transformer is included (Sec. 4.1) together with a discussion of correspondences with the dual filter (Sec. 4.3).

Remark 5 (Inference and learning) *The mathematics of the representation (1), derived here from first principles, provides a generalization of (Wiener filter-like) linear predictors to (transformer-like) nonlinear predictors. The HMM is a mathematically tractable model class for which this derivation is carried out. Solving the associated inference problem optimally is seen as the first step towards understanding how to learn these representations from data.*

1.4 Relevant literature

In contrast to the time-ordered structure of an HMM, the operations in a transformer are designed to exhibit a permutation symmetry: shuffling the past data (up to time t) does not affect the prediction at time t (Remark 16). For this reason, many studies view the ‘states’ in a transformer as (exchangeable) particles interacting through the attention mechanism, which has a certain interpretation as a nonlinear expectation. This perspective informs the modeling of transformer dynamics across layers (Yun et al., 2019; Vuckovic et al., 2020; Sander et al., 2022). Taking a continuous approximation of the discrete layers leads to an interacting particle ordinary differential equation (ODE) model of the transformer. For the analysis of such ODE models, it is natural to adopt a mean-field viewpoint and study a continuity equation on the space of probability measures (Geshkovski et al., 2023, 2024; Abella et al., 2024; Adu and Gharesifard, 2024; Castin et al., 2025).

Our objective is not to construct a mathematical model of a transformer, although this remains an important project. Rather, our interest lies in deriving, from first principles, transformer-like architectures that solve the prediction problem for which the transformer is designed. Specifically, our analysis leads to the dual-filter algorithm. We explicitly relate this algorithm to:

1. the transformer, including both its architecture and its attention mechanism (Sec. 4.1), and
2. the mathematical formalisms, specifically around modeling of a transformer as a transport on the space of probability measures, developed in prior mathematical frameworks (Remark 4.4).

Many authors have considered architectures that combine aspects of transformers with HMMs and filtering; see, e.g., Liu et al. (2022); Tang and Matteson (2021); Rohekar et al. (2023); Zhang and Feng (2023); Azeraf et al. (2021); Wang et al. (2018, 2021); Goel and Bartlett (2024); Chen et al. (2026). Also relevant are papers that adopt a Bayesian viewpoint (Xie et al., 2021; Han et al., 2023; He and Su, 2024; Ziemann et al., 2024; Ren et al., 2021; Ildiz et al., 2024), as well as those that explore control-theoretic properties of the transformer (Kong et al., 2024; Soatto et al., 2023; Liu et al.; Bhargava et al., 2023; Luo et al., 2023). Our approach differs from these works, which focus on interpreting and refining attention mechanisms, rather than modeling the prediction problem from first principles based on the representation in (1).

There is a large body of literature on variational methods for statistical inference for graphical models including HMMs (Jordan et al., 1999; Barber et al., 2011; McGoff et al., 2015; Bruna and Hsu, 2025). The optimal control-type variational problems introduced here are of fundamentally different nature. The differences are discussed in the main body of this paper (Sec. 2.5) after the optimal control problem has been formally introduced.

1.5 Outline of the remainder of this paper

The remainder of this paper is organized as follows: Sec. 2 presents the optimal control approach, beginning with the well-posedness of the representation (1) and concluding with the statement of

Symbol	Description
Spaces	
\mathbb{T}	Time-horizon: $\{0, 1, 2, \dots, T\}$ with $T < \infty$.
\mathbb{S}	State space: Finite set $\{1, 2, \dots, d\}$.
\mathbb{O}	Observation space (vocabulary): Finite set $\{0, 1, 2, \dots, m\}$.
Model parameters	
μ	Prior ($d \times 1$ probability vector).
A	Markov transition matrix (row stochastic $d \times d$ matrix).
C	Emission matrix (row stochastic $d \times (m + 1)$ matrix).
Other parameters	
c	$c(x)$ is a $m \times 1$ vector for each $x \in \mathbb{S}$ (it is obtained from C).
Γ	$\Gamma: \mathbb{R}^d \rightarrow \mathbb{R}^d$ (it is obtained from A).
R	$R(x)$ is a $m \times m$ matrix for each $x \in \mathbb{S}$ (it is obtained from C).

Table 1: Nomenclature for the HMM.

an explicit formula for U . Sec. 3 presents the fixed-point equation and its solution using the dual filter algorithm. Sec. 4 relates the dual filter to the decoder-only transformer and to prior measure-transport formalisms. Sec. 5 presents numerical results, and Sec. 6 concludes with a summary and directions for future work. All proofs are collected in the Appendix.

2 Optimal Control Theory: Formula for U

Concerning the representation (1), we begin with a well-posedness result.

Proposition 6 *For each $F \in \mathcal{Z}_T$ there exists a \mathcal{Z} -adapted process U such that (1) holds.*

Proof See Appendix A.1 where additional discussion is included concerning uniqueness of U (uniqueness requires additional assumptions on the HMM (μ, A, C)). ■

Our goal in this section is to describe an explicit formula for U . For this purpose, recall first that the conditional expectation has the following interpretation as the solution of the minimum mean-squared-error (MMSE) optimization problem:

$$\mathbb{E}(|F(X_T) - \pi_T(F)|^2) = \min\{\mathbb{E}(|F(X_T) - S|^2) : S \in \mathcal{Z}_T\}.$$

The technical considerations of this section are based on expressing the MMSE objective as an optimal control objective. We begin with some preliminaries.

2.1 Preliminaries: Martingale increment processes

Define

$$c(x) := \begin{bmatrix} C(x, 1) - C(x, 0) \\ C(x, 2) - C(x, 0) \\ \vdots \\ C(x, m) - C(x, 0) \end{bmatrix}_{m \times 1}, \quad x \in \mathbb{S}.$$

Symbol	Description
C	C is $d \times 2$ row stochastic matrix (same notation for the general m case).
c^+	$c^+(x) = C(x, 1)$ for each $x \in \mathbb{S}$.
c^-	$c^-(x) = C(x, 0)$ for each $x \in \mathbb{S}$.
c	$c(x) = c^+(x) - c^-(x)$ for each $x \in \mathbb{S}$ (same notation for the general m case).
r	$r(x) = (1 - c^2(x))$ for each $x \in \mathbb{S}$ (For $m > 1$, this is denoted by $R(x)$).

 Table 2: Nomenclature for the binary-valued HMM ($m = 1$ and $\mathbb{O} = \{0, 1\}$).

For each fixed $x \in \mathbb{S}$, $c(x)$ is a $m \times 1$ vector. The notation is useful to introduce the two \mathcal{F} -martingale increment processes associated with $(X, e(Z))$ as follows:

$$\begin{aligned} B_{t+1}(f) &:= f(X_{t+1}) - (Af)(X_t), \quad f \in \mathbb{R}^d, \quad t = 0, 1, 2, \dots, T-1, \\ W_{t+1} &:= e(Z_{t+1}) - c(X_t), \quad t = 0, 1, 2, \dots, T-1. \end{aligned}$$

The time indexing is used so that the processes are adapted with respect to \mathcal{F} (e.g., $W_t \in \mathcal{F}_t$ and $B_t \in \mathcal{F}_t$). Note we do not use the customary “ Δ ” notation to denote the increment processes. The notation is consistent with the model considered in (Elliott et al., 2008, Chapter 2).

For these processes, the formulae for conditional moments are given in the following proposition:

Proposition 7 *Consider B and W . Then*

$$\begin{aligned} \mathbb{E}(B_{t+1}(f) \mid \mathcal{F}_t \vee \mathcal{Z}_{t+1}) &= 0, \quad \mathbb{E}(|B_{t+1}(f)|^2 \mid \mathcal{F}_t \vee \mathcal{Z}_{t+1}) = (\Gamma f)(X_t), \quad \text{P-a.s.}, \quad f \in \mathbb{R}^d, \quad t = 0, 1, 2, \dots, T-1, \\ \mathbb{E}(W_{t+1} \mid \mathcal{F}_t) &= 0, \quad \mathbb{E}(W_{t+1}W_{t+1}^\top \mid \mathcal{F}_t) = R(X_t), \quad \text{P-a.s.}, \quad t = 0, 1, 2, \dots, T-1, \end{aligned}$$

where

$$\begin{aligned} (\Gamma f)(x) &:= \sum_{y \in \mathbb{S}} A(x, y) f^2(y) - (Af)^2(x), \quad x \in \mathbb{S}, \\ R(x) &:= \text{diag}(c(x)) + C(x, 0)(I + 11^\top) - c(x)c^\top(x), \quad x \in \mathbb{S}. \end{aligned}$$

Proof See Appendix B. ■

For reference, the nomenclature for the various HMM-related parameters is summarized in Table 1.

Example 2 (m=1) *Consider the HMM with binary-valued observations where $e(1) = 1$ and $e(0) = -1$. For this model, it is convenient to introduce notation*

$$c^+(x) := C(x, 1), \quad c^-(x) := C(x, 0), \quad x \in \mathbb{S}.$$

Note, $c^\pm(x) = \mathbb{P}(e(Z_{t+1}) = \pm 1 \mid X_t = x)$. For each fixed $x \in \mathbb{S}$, $c^+(x) + c^-(x) = 1$. Then

$$c(x) = C(x, 1) - C(x, 0) = c^+(x) - c^-(x), \quad x \in \mathbb{S}.$$

Likewise, $R(x)$ is now a scalar. The scalar is denoted by $R(x) = r(x)$, and given by

$$r(x) = C(x, 1) + C(x, 0) - c^2(x) = c^+(x) + c^-(x) - c^2(x) = (1 - c^2(x)), \quad x \in \mathbb{S}.$$

The nomenclature for the binary-valued HMM is included in Table 2.

Symbol	Description
HMM	
X	State process: $\{X_0, X_1, \dots, X_T\}$ is \mathbb{S} -valued.
Z	Observation process: $\{Z_1, Z_2, \dots, Z_T\}$ is \mathbb{O} -valued.
B	Process noise: $\{B_1, B_2, \dots, B_T\}$ is \mathbb{R}^d -valued.
W	Observation noise: $\{W_1, W_2, \dots, W_T\}$ is \mathbb{R}^m -valued.
Nonlinear filter	
π	Conditional measure: $\{\pi_0, \pi_1, \pi_2, \dots, \pi_T\}$ with $\pi_0 = \mu$ is $\mathcal{P}(\mathbb{S})$ -valued.
p	Prediction: $\{p_1, p_2, \dots, p_T\}$ is $\mathcal{P}(\mathbb{O})$ -valued.
BSΔE	
U	Control input: $\{U_0, U_1, \dots, U_{T-1}\}$ is \mathbb{R}^m -valued.
(Y, V)	Solution pair: $\{Y_0, Y_1, \dots, Y_{T-1}, Y_T\}$ with $Y_T = F$ is \mathbb{R}^d -valued. $\{V_0, V_1, \dots, V_{T-1}\}$ is $\mathbb{R}^{m \times d}$ -valued.

Table 3: Nomenclature for the stochastic processes.

2.2 Function spaces

The function spaces are as follows:

$$\begin{aligned} \mathcal{Y} &:= \{Y : \Omega \times \mathbb{T} \rightarrow \mathbb{R}^d, Y_t \in \mathcal{Z}_t, t \in \mathbb{T}\}, \\ \mathcal{V} &:= \{V : \Omega \times \{0, 1, 2, \dots, T-1\} \rightarrow \mathbb{R}^{m \times d}, V_t \in \mathcal{Z}_t, 0 \leq t \leq T-1\}, \\ \mathcal{U} &:= \{U : \Omega \times \{0, 1, 2, \dots, T-1\} \rightarrow \mathbb{R}^m, U_t \in \mathcal{Z}_t, 0 \leq t \leq T-1\}. \end{aligned}$$

\mathcal{Y} is the space of function-valued \mathcal{Z} -adapted stochastic processes (at time t , Y_t is a random function on \mathbb{S}). Likewise, \mathcal{V} is the space of matrix-valued \mathcal{Z} -adapted stochastic processes (at time t , each row of the matrix V_t is a random function on \mathbb{S}). \mathcal{U} is the space of admissible control inputs. (It is noted that \mathcal{U} is defined only for time indices $t = 0, 1, 2, \dots, T-1$, whereby, in (1), the control U_{t-1} is the weight for the t -th observation $e(Z_t)$, for a total of T -many weights for T -many observations.)

Based on Prop. 6, our goal is to find an element $U \in \mathcal{U}$ such that the representation (1) holds. To this end, we introduce an optimal control problem that involves two key components:

1. A definition of the dynamic constraint, and
2. A definition of the optimal control objective.

These are described in detail below, followed by a statement of the duality principle that links the filtering objective (MMSE) to the optimal control problem.

2.3 Dual optimal control problem

1. Dynamic constraint: is a backward stochastic difference equation (BSΔE)

$$Y_t(x) = (AY_{t+1})(x) + c^T(x)(U_t + V_t(x)) - V_t^T(x)e(Z_{t+1}), \quad x \in \mathbb{S}, \quad t = 0, 1, 2, \dots, T-1, \quad (2a)$$

$$Y_T(x) = F(x), \quad x \in \mathbb{S}. \quad (2b)$$

Here $U := \{U_t : 0 \leq t \leq T-1\} \in \mathcal{U}$ is an \mathbb{R}^m -valued stochastic process referred to as the control input and $F \in \mathcal{Z}_T$ is a \mathbb{R}^d -valued random vector referred to as the terminal condition. For a given control input $U \in \mathcal{U}$ and the terminal condition $F \in \mathcal{Z}_T$, the problem is to obtain a pair of \mathcal{Z} -adapted stochastic processes,

$$\begin{aligned} Y &:= \{Y_t(x) : Y_t(x) \in \mathcal{Z}_t, x \in \mathbb{S}, 0 \leq t \leq T\}, \\ V &:= \{V_t(x) : V_t(x) \in \mathcal{Z}_t, x \in \mathbb{S}, 0 \leq t \leq T-1\}, \end{aligned}$$

where for each fixed $x \in \mathbb{S}$, $Y_t(x)$ is real-valued and $V_t(x)$ is \mathbb{R}^m -valued. The pair is denoted by (Y, V) and referred to as the solution of the BSΔE (2). As stated, (2) is an example of a BSΔE on a lattice, the general theory for which appears in (Fukasawa et al., 2025). Based on this theory, we have the following well-posedness result:

Proposition 8 *Suppose $U \in \mathcal{U}$ and $F \in \mathcal{Z}_T$. Then there exists a unique $(Y, V) \in \mathcal{Y} \times \mathcal{V}$ that solves (2).*

Proof See Appendix A.2. The proof is self-contained based on adapting theory from (Fukasawa et al., 2025). ■

For reference, the nomenclature for the three different types of stochastic processes introduced thus far is given in Table 3.

2. Optimal control objective: Fix $U \in \mathcal{U}$. For the solution (Y, V) of the BSΔE (2), define

$$J_T(U; F) := \text{var}(Y_0(X_0)) + \mathbb{E}\left(\sum_{t=0}^{T-1} l(Y_{t+1}, V_t, U_t; X_t)\right),$$

where $\text{var}(Y_0(X_0)) = \mathbb{E}(|Y_0(X_0) - \mu(Y_0)|^2) = \mu(Y_0^2) - \mu(Y_0)^2$ (note here Y_0 is a deterministic function), and the running cost $l : \mathbb{R}^d \times \mathbb{R}^{m \times d} \times \mathbb{R}^m \times \mathbb{S} \rightarrow \mathbb{R}$ is given by,

$$l(y, v, u; x) := (\Gamma y)(x) + (u + v(x))^T R(x)(u + v(x)), \quad y \in \mathbb{R}^d, v \in \mathbb{R}^{m \times d}, u \in \mathbb{R}^m, x \in \mathbb{S}.$$

Here, $v(x)$ is the x -th column vector of the $m \times d$ matrix $v = [v(1) \ \cdots \ v(x) \ \cdots \ v(d)]_{m \times d}$.

Now that the dynamic constraint and the optimal control objective have been defined, the duality principle is given in the following theorem.

Theorem 9 (Duality principle) *Let $U \in \mathcal{U}$ and $F \in \mathcal{Z}_T$. Consider an estimator*

$$S_T := \mu(Y_0) - \sum_{t=1}^T U_{t-1}^T e(Z_t).$$

Then

$$J_T(U; F) = \mathbb{E}(|F(X_T) - S_T|^2).$$

Proof See Appendix C. ■

Noting that the right-hand side is the mean-squared error, the duality principle provides an optimal control approach to compute the conditional expectation.

• **Dual optimal control problem (OCP):**

$$\min_{U \in \mathcal{U}} J_T(U; F) \quad \text{subject to} \quad (2) \quad (3)$$

The following proposition is a corollary of Prop. 6 and helpful to relate the optimal control input, solution to (3), to the desired representation (1).

Proposition 10 *Consider OCP (3). For this problem, there exists an optimal control $U^{(\text{opt})} = \{U_t^{(\text{opt})} : 0 \leq t \leq T-1\} \in \mathcal{U}$ such that*

$$\pi_T(F) = \mu(Y_0^{(\text{opt})}) - \sum_{t=1}^T (U_{t-1}^{(\text{opt})})^\top e(Z_t), \quad \text{P-a.s.},$$

where $Y_0^{(\text{opt})}$ is obtained from solving the BSΔE (2) with $U = U^{(\text{opt})}$. The optimal value is given by

$$J_T(U^{(\text{opt})}; F) = \mathbb{E}(|F(X_T) - \pi_T(F)|^2) = \text{MMSE}.$$

Proof See Appendix D where Remark 20 is included concerning uniqueness of $U^{(\text{opt})}$. ■

2.4 Formula for optimal control

Notation: The following notation is introduced to denote the formula for optimal control:

$$\phi(y, v; \rho) := -\rho(R)^\dagger (\rho((c - \rho(c))y) - \rho(Rv)), \quad y \in \mathbb{R}^d, v \in \mathbb{R}^{m \times d}, \rho \in \mathcal{P}(\mathbb{S}).$$

Here, $\rho(R)^\dagger$ denotes the pseudo-inverse of the $m \times m$ matrix $\rho(R) := \sum_{x \in \mathbb{S}} \rho(x)R(x)$. The other two terms are $\rho((c - \rho(c))y) := \sum_{x \in \mathbb{S}} \rho(x)(c(x) - \rho(c))y(x)$ and $\rho(Rv) := \sum_{x \in \mathbb{S}} \rho(x)R(x)v(x)$. Note that both of these terms are $m \times 1$ vectors.

Let $u \in \mathbb{R}^m$ and $q \in \mathcal{P}(\mathbb{O})$. Denote

$$\langle u, u \rangle_q := q(0)(-1^\top u)^2 + \sum_{i=1}^m q(i)(u(i))^2 - \left(q(0)(-1^\top u) + \sum_{i=1}^m q(i)u(i) \right)^2.$$

The right-hand side is the variance of the function $\begin{bmatrix} (-1^\top u) \\ u \end{bmatrix} \in \mathbb{R}^{m+1}$ with respect to the probability vector q . By Jensen's inequality, $\langle u, u \rangle_q = 0$ implies $u(z) = \text{constant}$ for all such $z \in \mathbb{O}$ with $q(z) > 0$. If moreover $q(0) > 0$, then the constant must be zero.

Theorem 11 *Consider the OCP (3). Then an optimal control is of the feedback form given by*

$$U_t^{(\text{opt})} = \phi(Y_t, V_t; \pi_t), \quad \text{P-a.s.}, \quad 0 \leq t \leq T-1. \quad (4a)$$

For any $U \in \mathcal{U}$,

$$J_T(U; F) = \underbrace{\mathbb{E}(|F(X_T) - \pi_T(F)|^2)}_{\text{MMSE}} + \mathbb{E} \left(\sum_{t=0}^{T-1} \langle (U_t - U_t^{(\text{opt})}), (U_t - U_t^{(\text{opt})}) \rangle_{p_t} \right), \quad (4b)$$

where $p_t = \pi_t(C)$. Suppose $(Y^{(\text{opt})}, V^{(\text{opt})})$ is the solution of the BSΔE (2) with $U = U^{(\text{opt})}$. Then the following representation holds:

$$\pi_t(Y_t^{(\text{opt})}) = \mu(Y_0^{(\text{opt})}) - \sum_{s=1}^t (U_{s-1}^{(\text{opt})})^\top e(Z_s), \quad \text{P-a.s.}, \quad 1 \leq t \leq T. \quad (4c)$$

Proof See Appendix E. Concerning uniqueness, the formula (4a) identifies *one* optimal control input and (4b) provides a characterization of *all* such U for which the representation in (1) holds. The optimal control is unique iff $p_t(z) > 0$, P-a.s., $\forall z \in \mathbb{O}$, and $\forall t \in \mathbb{T}$. A sufficient condition is $\min\{C(x, z) : x \in \mathbb{S}, z \in \mathbb{O}\} > 0$ (see also Remark 20 in Appendix). ■

The most significant implication of this theorem is captured in the following remark:

Remark 12 (Fixed-point representation of conditional measure π) Compare (4c) with the representation given in Prop. 10. While the representation in Prop. 10 is given only for the terminal time T , Thm. 11 shows that the optimal control input yields a causal representation for the entire conditional measure $\pi = \{\pi_t : 0 \leq t \leq T\}$. Moreover, because the optimal control $U_t^{(\text{opt})}$ is a function of π_t (via the formula (4a)), (4c) is a fixed-point representation of π .

There are three problems in directly applying (4c) for computational purposes:

1. To compute the optimal control input, one needs to first compute π . This, however, somewhat undermines the original objective, as the primary goal of the algorithm is to compute π !
2. The solution procedure involves solving the BSΔE as an intermediate step. However, finding numerical solutions to the BSΔE is a challenging task, even in low-dimensional settings.
3. In applications of current interest, m is often large. For instance, in transformer models, a typical vocabulary size is $m \approx 100K$. The computation of optimal control using the formula for ϕ has a complexity $O(m^3)$, which becomes prohibitive for large m .

An analysis is presented in the following section that resolves these three challenges and yields a practical algorithm. For this purpose, the following corollary of Thm. 11 is useful.

Corollary 13 Consider the OCP (3) for $m = 1$ and $T = 1$. Then

$$U_0^{(\text{opt})} = \begin{cases} \frac{-1}{(1-\mu(c)^2)} (\mu((Af)(c - \mu(c))) - (\mu(A\tilde{f}) - \mu((A\tilde{f})c)\mu(c))), & 1 - \mu(c)^2 \neq 0, \\ 0 & \text{o.w.}, \end{cases} \quad (5)$$

where $f(x) = \frac{F^+(x) + F^-(x)}{2}$ and $\tilde{f}(x) = \frac{F^+(x) - F^-(x)}{2}$. For any admissible (deterministic) value of U_0 ,

$$J_1(U_0; F) = \underbrace{\mathbb{E}(|F(X_1) - \pi_1(F)|^2)}_{\text{MMSE}} + (1 - \mu(c)^2)(U_0 - U_0^{(\text{opt})})^2.$$

Proof See Appendix F. Although stated here as a corollary, the Appendix contains a self-contained formulation of the OCP and derivation of the formula (5). The derivation is useful to obtain an intuitive understanding of the general result in its simplest possible setting. ■

2.5 Related literature

Relationship to BSΔE literature: The form of the BSΔE considered in this paper is borrowed from Fukasawa et al. (2025). The paper introduces the coordinates $e : \mathbb{O} \rightarrow \mathbb{R}^m$ which are referred to as the lattice coordinates. Using these coordinates, existence and uniqueness theory for general types of BSΔE is given together with its application to finance. The BSΔE (2) is a special case of the general form considered in Fukasawa et al. (2025). The special form is introduced for the express purpose of deriving the nonlinear predictor (1) for an HMM. In particular, both the optimal control problem (Thm. 9) and its solution (Thm. 11) are original contributions of this paper.

Relationship to variational inference: For probabilistic graphical models, a standard way to cast inference as an optimization problem is through variational inference (VI), which formulates an entropy-type objective (Jordan et al., 1999), (Wainwright and Jordan, 2008, Sec. 3), and (Koller and Friedman, 2009, Ch. 11): Let $P_{X,Z}(\cdot, \cdot)$ denote the joint probability law of the stochastic process (X, Z) (which may be more general than the HMM considered here), and let $Z = z$ denote a fixed realization of the observations. In VI, the goal is to approximate the conditional law $P_{X|Z}(\cdot | Z = z)$ by selecting a law $P_X^\theta(\cdot)$ from a parameterized family so as to minimize the so-called *free energy* defined as follows:

$$\text{Free energy}(\theta) := \sum_x P_X^\theta(x) \log \frac{P_X^\theta(x)}{P_{X,Z}(x, z)}.$$

Since $P_{X|Z}(x | z) = P_{X,Z}(x, z)/P_Z(z)$, minimizing the free energy is equivalent (up to the additive constant $\log P_Z(z)$) to minimizing the Kullback–Leibler divergence $D(P_X^\theta \| P_{X|Z}(\cdot | z))$. The negative of the free energy is referred to as the *evidence lower bound (ELBO)*. Its maximum possible value is given by $\log P_Z(z)$. This maximum value is attained if and only if $P_X^{\theta^{(\text{opt})}}(\cdot) = P_{X|Z}(\cdot | Z = z)$, in which case VI yields exact inference.

For an HMM, when the variational family is unrestricted over the hidden state sequence, the ELBO is achieved at its maximum and VI is exact. In this case, the optimal marginal distribution at time $t = T$ coincides with the filtering posterior π_T .

VI-based dual optimal control formulations: For certain classes of HMMs—notably stochastic differential equation (SDE) models in continuous-time with additive white noise observations (see Xiong (2008))—the VI objective based on the divergence minimization can be expressed as an optimal control-type objective. This equivalence is obtained by parameterizing the approximating law $P^\theta(X)$ as the law of a controlled stochastic process; see (Mitter and Newton, 2003, Sec. 3) for the case where X is an Itô diffusion and (van Handel, 2006, Sec. 2.2) for the case where X is a discrete-valued continuous-time Markov process. The resulting optimal control problem is a generalization of the classical Mortensen’s maximum-likelihood estimator (Mortensen, 1968), also referred to as minimum energy duality (Hijab, 1980). Related papers on this topic include (Todorov, 2008; Sutter et al., 2016; Kim and Mehta, 2020; Raginsky, 2024).

In contrast, the optimal control formulation developed in the present work generalizes Kalman’s minimum variance duality, which is based on MMSE rather than the divergence-type objective. The terminology “minimum variance duality” and “minimum energy duality” follows Bensoussan (Bensoussan, 2018, p. 180). As noted in (Kailath et al., 2000, p. 100), these two duality principles are not directly related in general, despite yielding identical solutions in the linear Gaussian model. Prior to our work (Kim et al., 2019a), it was widely believed that minimum variance duality could not be extended beyond the LQG setting; see, for example, Todorov (2008), who wrote:

“Kalman’s duality has been known for half a century and has attracted a lot of attention. If a straightforward generalization to non-LQG settings was possible it would have been discovered long ago. Indeed, we will now show that Kalman’s duality, although mathematically sound, is an artifact of the LQG setting.”

The present paper provides, to our knowledge, the first extension of minimum variance duality to discrete-time HMMs with discrete-valued observations. The derivation is based on suitably adapting original arguments from our prior work (Kim et al., 2019b; Kim and Mehta, 2024b) given there in the continuous-time settings of the model. For this purpose, the key technical tool employed here is the BSΔE theory developed in (Fukasawa et al., 2025).

There are two reasons for considering Kalman’s minimum variance duality:

1. Kalman’s duality is structurally fundamental from a control-theoretic perspective. This is so because the MMSE objective is directly tied to the structural duality between observability and controllability (Callier and Desoer, 2012, Ch. 8). In particular, the HMM (μ, A, C) is observable if and only if the BSΔE (2) is controllable (Kim and Mehta, 2024a). From a theoretical standpoint, this property is useful for the purposes of filter stability analysis (Kim and Mehta, 2024c; Kim et al., 2024).
2. From a practical standpoint, the OCP (3) is useful to design the optimal weights in the non-linear predictor (1).

A historical overview of duality theory in control and estimation is provided in (Kim and Mehta, 2025).

3 Fixed-point equation: Dual filter algorithm

Consider a fixed sample path of observations $z := [z_1, z_2, \dots, z_T] \in \mathbb{O}^T$ such that $P(Z = z) > 0$ (such a sample path is an input to a transformer). The conditional measure for this fixed sample path is denoted by

$$\pi^{(z)} := [\pi_1^{(z)}, \pi_2^{(z)}, \dots, \pi_T^{(z)}] \in \mathcal{P}(\mathbb{S})^T \quad \text{where} \quad \pi_t^{(z)}(x) = P(X_t = x | Z_1 = z_1, \dots, Z_t = z_t), \quad x \in \mathbb{S}, \quad 1 \leq t \leq T.$$

Our objective in this section is to define a layer transformation

$$\mathcal{N}^{(\text{dfftr})} : \mathcal{P}(\mathbb{S})^T \mapsto \mathcal{P}(\mathbb{S})^T \quad \text{such that} \quad \pi^{(z)} = \mathcal{N}^{(\text{dfftr})}(\pi^{(z)}).$$

(The $d \times T$ input and output data structures are the same as those of a transformer layer.)

For the purpose of defining the layer transformation $\mathcal{N}^{(\text{dfftr})}$, consider first a model for binary-valued observations as follows:

$$c_t^+(x) := C(x, z_t), \quad c_t^-(x) := 1 - C(x, z_t), \quad c_t(x) := c_t^+(x) - c_t^-(x), \quad x \in \mathbb{S}, \quad 1 \leq t \leq T.$$

Let $\rho = [\rho_1, \rho_2, \dots, \rho_T] \in \mathcal{P}(\mathbb{S})^T$. Consider a deterministic backward difference equation (BΔE) as follows:

$$y_t(x) = (Ay_{t+1})(x) + c_{t+1}(x)u_t, \quad x \in \mathbb{S}, \quad t = 0, 1, 2, \dots, T-1, \quad (6a)$$

$$u_t = \begin{cases} \phi(y_t, 0; \rho_t), & t = 1, 2, \dots, T-1, \\ \phi(y_t, 0; \mu), & t = 0, \end{cases} \quad (6b)$$

$$y_T(x) = f(x), \quad x \in \mathbb{S}, \quad (6c)$$

where the control input $u = \{u_t \in \mathbb{R} : 0 \leq t \leq T-1\}$ and the solution $y = \{y_t(x) \in \mathbb{R} : x \in \mathbb{S}, 0 \leq t \leq T\}$ are both deterministic processes (the lower-case notation is used to stress this). Note that the control input is obtained using the formula ϕ for optimal control with a given measure ρ_t .

Because the terminal condition $y_T = f$ is arbitrary, the solution y defines a measure-valued process $\rho^+ = [\rho_1^+, \rho_2^+, \dots, \rho_T^+] \in \mathcal{M}(\mathbb{S})^T$ as follows:

$$\rho_t^+(y_t) := \mu(y_0) - \sum_{s=1}^t u_{s-1}, \quad 1 \leq t \leq T, \quad (6d)$$

where on the right-hand side, $\{u_s \in \mathbb{R} : 0 \leq s \leq t-1\}$ is according to (6b) and y_0 is the solution of (6a) at time $t=0$. It is clear that $\rho_t^+ \in \mathcal{M}(\mathbb{S})$ because the right-hand side of (6d) is well-defined for each $t = 1, 2, \dots, T$. The layer transformation for the dual filter is now defined as follows:

$$\mathcal{N}^{(\text{dfftr})} : \mathcal{D} \subset \mathcal{P}(\mathbb{S})^T \mapsto \mathcal{P}(\mathbb{S})^T \quad \text{as} \quad \mathcal{N}^{(\text{dfftr})}(\rho) := \rho^+,$$

where the domain \mathcal{D} is defined to be the largest subset in $\mathcal{P}(\mathbb{S})^T$ such that $\mathcal{N}^{(\text{dfftr})}\rho \in \mathcal{P}(\mathbb{S})^T$. That the domain is non-empty is because of the following proposition which also shows the significance of (6) to the computation of $\pi^{(z)}$.

Proposition 14 *Consider (6). Then $\pi^{(z)} \in \mathcal{D}$ and moreover*

$$\mathcal{N}^{(\text{dfftr})}(\pi^{(z)}) = \pi^{(z)}.$$

Proof See Appendix G. ■

The result lays the foundation for a practical algorithm described next. At its core, the algorithm implements the mapping $\mathcal{N}^{(\text{dfftr})}$.

3.1 Algorithms

In the following, we describe two algorithms to approximate the solution of the fixed-point equation:

1. An iterative algorithm.
2. A single-shot algorithm.

The iterative algorithm is useful to obtain a correspondence with the transformer. The single-shot algorithm is more efficient, and requires only a single iteration. The pseudocodes for all the algorithms described in this section appear in Appendix H.

1. Iterative algorithm:

1. Initialize $\rho^{(0)} = \{\rho_t^{(0)} : 1 \leq t \leq T\} \in \mathcal{P}(\mathbb{S})^T$. Inspired from input used in a transformer, a reasonable choice is

$$\rho_t^{(0)}(x) = \frac{C(x, z_t)}{\sum_{x' \in \mathbb{S}} C(x', z_t)}, \quad x \in \mathbb{S}, \quad 1 \leq t \leq T.$$

2. Denote $\rho^{(\ell)} = \{\rho_t^{(\ell)} : 1 \leq t \leq T\} \in \mathcal{P}(\mathbb{S})^T$ for $\ell = 1, 2, \dots, L$. The dual filter (6) is simulated to compute

$$\rho^{(\ell+1)} = \text{Project}(\mathcal{N}^{(\text{dfftr})} \rho^{(\ell)}), \quad \ell = 0, 1, 2, \dots, L-1,$$

where $\text{Project}(\cdot)$ is used to ensure that the $\rho^{(\ell+1)} \in \mathcal{P}(\mathbb{S})^T$ (see Algorithm 5 in Appendix H).

3. At the final layer, the nonlinear predictor for the next observation is obtained as

$$p_t(z) = \mathbb{P}(Z_{t+1} = z | Z_1 = z_1, \dots, Z_t = z_t) = \rho_t^{(L)}(C) = \sum_{x \in \mathbb{S}} \rho_t^{(L)}(x) C(x, z), \quad t = 1, 2, \dots, T, \quad z \in \mathbb{O}.$$

Note the prediction is over the entire time horizon.

The pseudocode for the iterative algorithm is given in Algorithm 1 in Appendix H.

2. Single-shot algorithm: In contrast to the iterative algorithm, the single-shot algorithm requires only a single iteration for convergence. The difference between the two algorithms is as follows:

1. For the iterative algorithm, each iteration implements a single backward pass.
2. For the single-shot algorithm, there is only a single iteration which implements T backward passes, where the result of the t -th pass is used to compute the result of the $(t+1)$ -th pass.

Using the single-shot algorithm, after the t -th backward pass, the conditional measure is computed as follows:

$$\pi_t^{(z)}(f) = \mu(y_0) - \sum_{s=1}^t u_{s-1}, \quad 1 \leq t \leq T,$$

where the control $\{u_{s-1} : 1 \leq s \leq t\}$ are computed using the formula for the optimal control with measures $\{\mu, \pi_1^{(z)}, \dots, \pi_{t-1}^{(z)}\}$ (known from $(t-1)$ -th pass). From this, the prediction at time t is computed as $p_t(z) = \pi_t^{(z)}(C(\cdot, z))$. The pseudocode for the single-shot algorithm is given in Algorithm 2 in Appendix H.

An advantage of the single-shot algorithm is that the computation does not require multiple iterations. On the other hand, the iterative algorithm has structural similarities with the transformer architecture. These are described at length in the following subsection. Note that either of the algorithms is designed to numerically compute the fixed-point of $\mathcal{N}^{(\text{dfftr})}$, based on solving (6).

4 Relationship to transformer modeling

4.1 Input-output architecture

We begin by describing, in a self-contained manner, the architecture and the algorithmic operations inside a decoder-only transformer. The description is based upon (Phuong and Hutter, 2022) (Jurafsky and Martin, 2025, Ch. 10) and (Raschka, 2024).

In a decoder-only transformer, as a first step, a token is “embedded” using a $d \times m$ embedding matrix denoted in this paper by $C^{(\text{xfer})}$:

$$z \mapsto C^{(\text{xfer})}(\cdot, z) \in \mathbb{R}^d, \quad z \in \mathbb{O}.$$

Using the embedding matrix,

$$\begin{bmatrix} z_1 & \cdots & z_t & \cdots & z_T \end{bmatrix}_{1 \times T} \mapsto \begin{bmatrix} C^{(\text{xfer})}(:, z_1) & \cdots & C^{(\text{xfer})}(:, z_t) & \cdots & C^{(\text{xfer})}(:, z_T) \end{bmatrix}_{d \times T}.$$

The input $C^{(\text{xfer})}(:, z_t)$ is augmented with the so-called positional encoding as follows:

$$e_t(x) := C^{(\text{xfer})}(x, z_t) + W_p(x, t), \quad x \in \mathbb{S}, \quad t = 1, 2, \dots, T,$$

where $W_p \in \mathbb{R}^{d \times T}$ is referred to as the positional encoding matrix. In the original transformer paper (Vaswani et al., 2017), the rows of W_p are defined according to the sinusoidal-positional-encoding:

$$W_p(2i-1, t) = \sin(\ell_{\max}^{-\frac{2i}{d}} t), \quad W_p(2i, t) = \cos(\ell_{\max}^{-\frac{2i}{d}} t), \quad i = 1, 2, \dots, \frac{d}{2}, \quad t = 1, 2, \dots, T,$$

where $\ell_{\max} = 10,000$. The factor $\ell_{\max}^{-\frac{2i}{d}}$ determines the frequency of oscillations, ensuring a wide range of scales, as i varies from $1, 2, \dots, \frac{d}{2}$. The positional encoding is the *only* mechanism by which information about the position (time) t is introduced into the transformer. Other types of positional encoding are also possible (see Remark 15).

From an input-output perspective, a decoder-only transformer implements a causal nonlinear transformation that transforms a $d \times T$ matrix at the input into a $d \times T$ matrix at the output,

$$\begin{bmatrix} e_1 & \cdots & e_t & \cdots & e_T \end{bmatrix}_{d \times T} \mapsto \begin{bmatrix} \sigma_1^{(L)} & \cdots & \sigma_t^{(L)} & \cdots & \sigma_T^{(L)} \end{bmatrix}_{d \times T}.$$

From the output $\sigma_t^{(L)}$, the conditional probability of the next token is computed as follows:

$$p_t(z) = \text{P}(Z_{t+1} = z \mid Z_1 = z_1, \dots, Z_t = z_t) = \frac{e^{((\sigma_t^{(L)})^T C^{(\text{xfer})})(z)}}{\sum_{z' \in \mathbb{O}} e^{((\sigma_t^{(L)})^T C^{(\text{xfer})})(z')}}}, \quad t = 1, 2, \dots, T, \quad z \in \mathbb{O}.$$

The operation on the right-hand side is referred to as softmax.

Internally, a transformer is arranged in L layers as follows:

$$\text{(input)} \quad [z_1, z_2, \dots, z_T]_{1 \times T} \mapsto [e_1, e_2, \dots, e_T]_{d \times T} \quad (\text{embedding + positional-encoding})$$

$$\text{(first layer)} \quad [e_1, e_2, \dots, e_T]_{d \times T} \mapsto [\sigma_1^{(1)}, \sigma_2^{(1)}, \dots, \sigma_T^{(1)}]_{d \times T}$$

$$\text{(intermediate layer)} \quad [\sigma_1^{(\ell)}, \sigma_2^{(\ell)}, \dots, \sigma_T^{(\ell)}]_{d \times T} \mapsto [\sigma_1^{(\ell+1)}, \sigma_2^{(\ell+1)}, \dots, \sigma_T^{(\ell+1)}]_{d \times T}, \quad \ell = 1, 2, \dots, L-1$$

$$\text{(output)} \quad [\sigma_1^{(L)}, \sigma_2^{(L)}, \dots, \sigma_T^{(L)}]_{d \times T} \mapsto [p_1, p_2, \dots, p_T]_{m \times T} \quad (\text{un-embedding})$$

The correspondence between the dual filter (iterative) and the transformer is as follows:

1. Input:

$$\text{(dual filter)} \quad \rho_t^{(0)}(x) = \frac{C(x, z_t)}{\sum_{x' \in \mathbb{S}} C(x', z_t)}, \quad x \in \mathbb{S}, \quad 1 \leq t \leq T,$$

$$\text{(transformer)} \quad e_t(x) = C^{(\text{xfer})}(x, z_t) + W_p(x, t), \quad x \in \mathbb{S}, \quad 1 \leq t \leq T.$$

2. Layers:

$$\text{(dual filter)} \quad [\rho_1^{(\ell)}, \rho_2^{(\ell)}, \dots, \rho_T^{(\ell)}]_{d \times T} \mapsto [\rho_1^{(\ell+1)}, \rho_2^{(\ell+1)}, \dots, \rho_T^{(\ell+1)}]_{d \times T}, \quad \ell = 1, 2, \dots, L-1, \quad (8a)$$

$$\text{(transformer)} \quad [\sigma_1^{(\ell)}, \sigma_2^{(\ell)}, \dots, \sigma_T^{(\ell)}]_{d \times T} \mapsto [\sigma_1^{(\ell+1)}, \sigma_2^{(\ell+1)}, \dots, \sigma_T^{(\ell+1)}]_{d \times T}, \quad \ell = 1, 2, \dots, L-1. \quad (8b)$$

3. Output:

$$\text{(dual filter)} \quad p_t(z) = \sum_{x \in \mathbb{S}} \rho_t^{(L)}(x) C(x, z), \quad t = 1, 2, \dots, T, \quad z \in \mathbb{O},$$

$$\text{(transformer)} \quad \ln p_t(z) = \sum_{x \in \mathbb{S}} \sigma_t^{(L)}(x) C^{(\text{xfer})}(x, z) + (\text{constant}), \quad t = 1, 2, \dots, T, \quad z \in \mathbb{O}.$$

4.2 Layer operation in a transformer

Because each layer in a transformer is structurally identical, for the purposes of describing the mapping, it suffices to consider a generic layer whose input and output are denoted by,

$$\sigma := [\sigma_1, \sigma_2, \dots, \sigma_T]_{d \times T} \in \mathcal{M}(\mathbb{S})^T, \quad \sigma^+ := [\sigma_1^+, \sigma_2^+, \dots, \sigma_T^+]_{d \times T} \in \mathcal{M}(\mathbb{S})^T,$$

respectively, and the layer mapping is denoted by

$$\mathcal{N}^{(\text{xfer})} : \mathcal{M}(\mathbb{S})^T \mapsto \mathcal{M}(\mathbb{S})^T \quad \text{such that} \quad \sigma^+ = \mathcal{N}^{(\text{xfer})}(\sigma).$$

For the first layer, the input is given by the embedding plus positional encoding. For each subsequent layer, the input is defined by the output of the preceding layer.

Operationally, a layer is comprised of multiple attention heads. A single attention head is an input-output map of the form

$$[\sigma_1, \sigma_2, \dots, \sigma_T]_{d \times T} \mapsto [o_1^h, o_2^h, \dots, o_T^h]_{d_V \times T}.$$

where the output vector $o_t^h \in \mathbb{R}^{d_V}$ has dimension $d_V = \frac{d}{n_{\text{head}}}$, with n_{head} denoting the number of heads. The operations in a single attention head are defined by three matrices

$$W_V^h \in \mathbb{R}^{d_V \times d}, \quad W_Q^h \in \mathbb{R}^{d_K \times d}, \quad W_K^h \in \mathbb{R}^{d_K \times d},$$

where typically $d_K = d_V$. The matrices are constant (fixed) during the inference phase of the transformer operation.

The mathematical operation defining the *causal self-attention* is as follows:

$$o_t^h = W_V^h \left(\sum_{s=1}^t \alpha(s; t, h) \sigma_s \right), \quad t = 1, 2, \dots, T, \quad (10)$$

where $\{\alpha(s; t, h) : s = 1, 2, \dots, t\}$ is referred to as the attention weight vector. For each fixed $(t, h) \in \{1, 2, \dots, T\} \times \{1, 2, \dots, n_{\text{head}}\}$, it is a probability vector. That is,

$$\alpha(s; t, h) \geq 0, \quad s = 1, 2, \dots, t, \quad \text{and} \quad \sum_{s=1}^t \alpha(s; t, h) = 1.$$

The attention weights are computed as follows: For each fixed $1 \leq t \leq T$, define

$$\begin{aligned} \text{(query)} \quad q_t &= W_Q^h \sigma_t, \\ \text{(key)} \quad k_s &= W_K^h \sigma_s, \quad s = 1, 2, \dots, t. \end{aligned}$$

Then

$$\text{(attention weight)} \quad \alpha(s; t, h) = \frac{\exp(\frac{q_t^\top k_s}{\sqrt{d_K}})}{\sum_{\tau=1}^t \exp(\frac{q_t^\top k_\tau}{\sqrt{d_K}})}, \quad s = 1, 2, \dots, t.$$

Remark 15 (Attention as a nonlinear predictor) *Two remarks on the interpretation of attention as a nonlinear predictor are as follows:*

1. *In the terminology adopted in this paper, the dependence of the attention weights α_s^t upon the data (which varies between sample paths of observations), makes attention a nonlinear predictor. If the weights were deterministic (same for all sample paths), attention will be an example of a linear predictor (see Remark 1).*
2. *In the kernelized relative position encoding (RPE),*

$$\alpha_s^t = \text{softmax}\left(\frac{1}{\sqrt{d_K}} q_t^\top k_s + b(t-s)\right), \quad s = 1, 2, \dots, t,$$

where the function $b(\cdot)$ may be pre-specified (Press et al., 2021) or learned (Chi et al., 2022). By itself, without the $q_t^\top k_s$ term, the resulting predictor is linear.

Remark 16 (Properties of attention operation) *Two salient properties of attention are as follows:*

1. *Attention operation (10) is the only mechanism by which the input data e_s at other time indices ($s = 1, 2, \dots, t-1$) influences the output at time t . All other operations in the transformer are applied independently at each fixed t .*
2. *Attention operation (10) exhibits a symmetry: permuting the inputs $\{e_1, e_2, \dots, e_{t-1}\}$ (while keeping e_t fixed) yields the identical output y_t^h at time t .*

From (10), the layer output is obtained as

$$\sigma_t^+ = W_O \text{concat}(o_t^1, \dots, o_t^{n_{\text{head}}}), \quad t = 1, 2, \dots, T,$$

where $W_O \in \mathbb{R}^{d \times d}$.

A potential issue during the training phase of a transformer is that the output may ‘blow up’. For this reason, several miscellaneous operations are implemented. All of these operations are carried out independently for each fixed t . Because these operations are not especially pertinent to establishing the correspondence with the dual filter, they are described in Appendix I.

Concept	Probabilistic model	Surrogates in a transformer
State space	$\mathbb{S} = \{1, 2, \dots, d\}$	Dimension d of embedding vector
Observation space	$\mathbb{O} = \{0, 1, 2, \dots, m\}$	Vocabulary
Discrete-time	$\mathbb{T} = \{0, 1, 2, \dots, T\}$	T is context length
Observation process	$Z = [Z_1, Z_2, \dots, Z_T]$ is \mathbb{O} -valued	Token-ized prompt
Latent process	$X = [X_0, X_1, \dots, X_T]$ is \mathbb{S} -valued	Internal latent state in language
Observation model	$C(x, z) = P(Z_{t+1} = z X_t = x), x \in \mathbb{S}, z \in \mathbb{O}$	Embedding matrix $C^{(\text{xfer})}(x, z)$

Table 4: Probabilistic model and its surrogates in a transformer.

Concept	Inference architecture	Surrogates in a transformer
Layer operation		
Layer mapping	$\mathcal{N}^{(\text{dfftr})} : \mathcal{P}(\mathbb{S})^T \mapsto \mathcal{P}(\mathbb{S})^T$	$\mathcal{N}^{(\text{xfer})} : \mathcal{M}(\mathbb{S})^T \mapsto \mathcal{M}(\mathbb{S})^T$
Layer ℓ input	$\rho^{(\ell)}$	$\sigma^{(\ell)}$
Layer ℓ output	$\rho^{(\ell+1)} = \mathcal{N}^{(\text{dfftr})}(\rho^{(\ell)})$	$\sigma^{(\ell+1)} = \mathcal{N}^{(\text{xfer})}(\sigma^{(\ell)})$
Final layer output		
Cond. measure	$\pi = [\pi_1, \pi_2, \dots, \pi_T]$ is $\mathcal{P}(\mathbb{S})$ -valued	$\sigma^L = [\sigma_1^L, \sigma_2^L, \dots, \sigma_T^L]$ is $\mathcal{M}(\mathbb{S})$ -valued
Fixed-point	$\pi = \mathcal{N}^{(\text{dfftr})}(\pi)$	unknown
Prediction	$p_t(z) = \sum_x \pi_t(x) C(x, z), z \in \mathbb{O}$	$\ln p_t(z) = \sum_x \sigma_t^{(L)}(x) C^{(\text{xfer})}(x, z) + (\text{const})$

Table 5: Inference architecture and its surrogates in a transformer.

4.3 Correspondence between the layer operations

The layer operations in the dual filter and the transformer can be viewed abstractly as maps between sequences of measures. Fig. 2 illustrates this comparison for the two maps,

$$\begin{aligned}
 (\text{dual filter}) \quad & \mathcal{N}^{(\text{dfftr})} : \mathcal{P}(\mathbb{S})^T \mapsto \mathcal{P}(\mathbb{S})^T, \\
 (\text{transformer}) \quad & \mathcal{N}^{(\text{xfer})} : \mathcal{M}(\mathbb{S})^T \mapsto \mathcal{M}(\mathbb{S})^T.
 \end{aligned}$$

There are two structural similarities between these maps:

1. For both of these maps, the input and also the output at time t is a $d \times 1$ vector, for $t = 1, 2, \dots, T$.
2. The final layer output at time t is used to approximate the prediction p_t at time t .

For the dual filter, these properties follow from the probabilistic modeling which is closely inspired by the surrogates in the transformer (see Table 4). Note that there is no surrogate in the transformer for the state transition matrix A which is used here to model the latent process X as a Markov chain.

It is important to distinguish between the \mathbb{S} -valued latent process X and the Markov assumption imposed on it. The $\mathcal{P}(\mathbb{S})$ -valued conditional measure π and the nonlinear predictor (1) are well-defined even without assuming that X is Markov (see Remark 19 in Appendix A.1). The correspondence in Table 5 emphasizes the layer mapping and its role in computing π as a fixed point.

The Markov assumption is not a modeling claim about transformers. Its sole purpose here is analytic: it enables an explicit expression for the control U in (1), and hence an explicit form of the layer map $\mathcal{N}^{(\text{dfftr})}$. In this sense, the Markov model serves as a tractable baseline from which one can

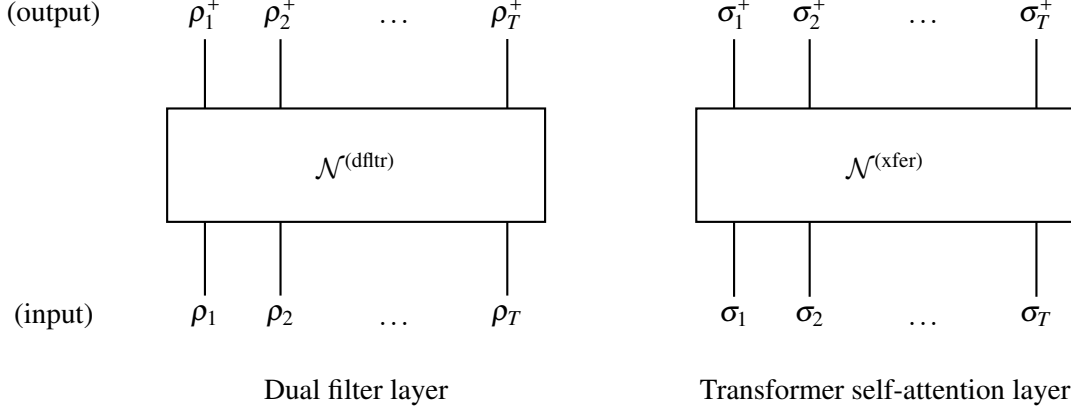


Figure 2: Structural correspondence between the dual filter layer and a self-attention layer in a decoder-only transformer. (left) The proposed layer map $\mathcal{N}^{(\text{dfltr})} : \rho \in \mathcal{P}(\mathbb{S})^T \mapsto \rho^+ \in \mathcal{P}(\mathbb{S})^T$. (right) A transformer layer $\mathcal{N}^{(\text{xfer})} : \sigma \in \mathcal{M}(\mathbb{S})^T \mapsto \sigma^+ \in \mathcal{M}(\mathbb{S})^T$. In both cases, the transformation maps a sequence of d -dimensional vectors to another sequence of d -dimensional vectors of the same length.

investigate principled modifications of the transition structure (see Alaa and van der Schaar (2019); Tang and Matteson (2021)) that move the architecture closer to modern attention-based models.

4.4 Comparison with prior modeling work

At the core of the dual filter is the mapping $\mathcal{N}^{(\text{dfltr})} : \mathcal{P}(\mathbb{S})^T \rightarrow \mathcal{P}(\mathbb{S})^T$ which defines a transport on the space of probability measures. This is contrasted with the mathematical modeling of a transformer described in (Geshkovski et al., 2023, 2024; Abella et al., 2024; Adu and Gharesifard, 2024; Castin et al., 2025). For this purpose, it is useful to first recall the input-output operation of a single layer (repeated from (8) above):

$$\begin{aligned}
 \text{(dual filter)} \quad & [\rho_1^{(\ell)}, \rho_2^{(\ell)}, \dots, \rho_T^{(\ell)}]_{d \times T} \mapsto [\rho_1^{(\ell+1)}, \rho_2^{(\ell+1)}, \dots, \rho_T^{(\ell+1)}]_{d \times T}, \quad \ell = 1, 2, \dots, L-1, \\
 \text{(transformer)} \quad & [\sigma_1^{(\ell)}, \sigma_2^{(\ell)}, \dots, \sigma_T^{(\ell)}]_{d \times T} \mapsto [\sigma_1^{(\ell+1)}, \sigma_2^{(\ell+1)}, \dots, \sigma_T^{(\ell+1)}]_{d \times T}, \quad \ell = 1, 2, \dots, L-1.
 \end{aligned}$$

The viewpoint espoused in these earlier studies is to regard $\sigma^\ell = \{\sigma_t^{(\ell)} : 1 \leq t \leq T\}$ as an ensemble. These are suitably normalized such that each ensemble member (particle) $\sigma_t^{(\ell)}$ is an element of the sphere $S^{d-1} := \{s \in \mathbb{R}^d : |s| = 1\}$ for $t = 1, 2, \dots, T$, and the ensemble defines an empirical measure in $\mathcal{P}(S^{d-1})$. The objective of the prior work is to study the nonlinear mapping $\sigma^\ell \mapsto \sigma^{\ell+1}$ as a transport on $\mathcal{P}(S^{d-1})$. For tractability, several simplifying assumptions are necessary. These include assuming an exchangeability property of the ensemble members (this property does not hold with causal masking), ignoring the effect of positional encoding, and taking a continuous approximation of the discrete layers in order to derive a continuity equation for the transport.

Summarizing, both our work and the prior studies provide mathematical frameworks to model and understand a transformer as a transport on an appropriate space of probability measures. Notably, the spaces are very different, $\mathcal{P}(\mathbb{S})^T$ for us and $\mathcal{P}(S^{d-1})$ for the prior work. Moreover, the approaches differ in focus. The prior work, because it explicitly models the attention mechanism as it is implemented, is more faithful to the actual architecture of the transformer. In contrast, our

work models the functional goal of the transformer—namely to predict the next token—rather than its detailed implementation.

5 Numerics with the dual filter

The numerical experiments are designed to validate the dual filter on a known HMM, where the parameters are chosen to mimic certain models of transformers. Specifically, we adopt parameter settings following the character-level configuration from Karpathy’s nanoGPT implementation (Karpathy, 2022): $d = 384$, $m = 65$, and $T = 256$. The HMM parameters (μ, A, C) are configured as follows:

- The prior μ is set to the uniform probability vector: $\mu(x) = \frac{1}{d}$ for $x \in \mathbb{S}$.
- The transition matrix A is a convex combination of two components: a cyclic permutation matrix $A^{(\text{circ})}$ (encoding a deterministic transition $0 \mapsto 1 \mapsto 2 \mapsto \dots \mapsto (d-1) \mapsto 0$) and a randomly sampled stochastic matrix $A^{(\text{stoch})}$,

$$A = \alpha A^{(\text{circ})} + (1 - \alpha) A^{(\text{stoch})}, \quad \text{where } A^{(\text{circ})}(x, x') = \begin{cases} 1, & x' = x + 1 \pmod{d}, \\ 0, & \text{o.w.} \end{cases}, \quad x, x' \in \mathbb{S}$$

where $\alpha \in (0, 1)$ is a homotopy parameter.

- The emission matrix C is randomly sampled. See Algorithm 7 for details.
- In both $A^{(\text{stoch})}$ and C , each row is sampled independently: row-entries are drawn i.i.d. from a standard Normal distribution and then normalized using the softmax operation to form a valid probability vector.

Spectral properties of the transition matrix A as a function of the homotopy parameter α are illustrated in Fig. 3.

5.1 Dual filter algorithm

An observation sequence $\{z_1, z_2, \dots, z_T\}$ is a single sample path generated from the HMM defined by the parameters above with $\alpha = 1$. The ground truth is obtained by simulating the nonlinear filter (forward algorithm) to compute the conditional probability $p_t(z)$ at each time step $t \in \mathbb{T}$ and $z \in \mathbb{O}$. This is denoted by $p_t^{(\text{forward})}(z)$ and compared with the conditional probability computed using the two dual filter algorithms:

1. Fig. 4 depicts the comparison with the single-shot algorithm.
2. Fig. 5 depicts the comparison with the iterative algorithm.

The following error metric is used to help illustrate the convergence,

$$\varepsilon_t^{(\ell)} := \varepsilon(p_t^{(\ell)}; p_t^{(\text{forward})}), \quad \varepsilon(p'; p) := \max_{z \in \mathbb{O}} |p'(z) - p(z)|, \quad \ell = 1, 2, \dots, L.$$

For the single-shot algorithm, only a single iteration is necessary, and therefore, $L = 1$. In what follows, all computations are carried out with the single-shot algorithm.

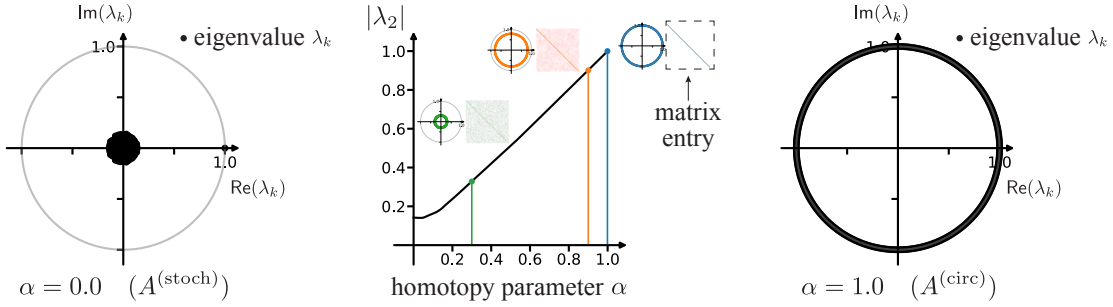


Figure 3: Eigenvalues of the transition matrix A as a function of the homotopy parameter α . (Middle): Plot of the second eigenvalue magnitude $|\lambda_2|$ as a function of α . (Left): Eigenvalue spectrum for $A = A^{(\text{stoch})}$ ($\alpha = 0$). (Right): Eigenvalue spectrum for $A = A^{(\text{circ})}$ ($\alpha = 1$). In the middle plot, three representative values of α —0.3 (green), 0.9 (orange), and 1.0 (blue)—are highlighted. Insets show the corresponding eigenvalue spectra and matrix structures; darker shades indicate higher matrix entry values.

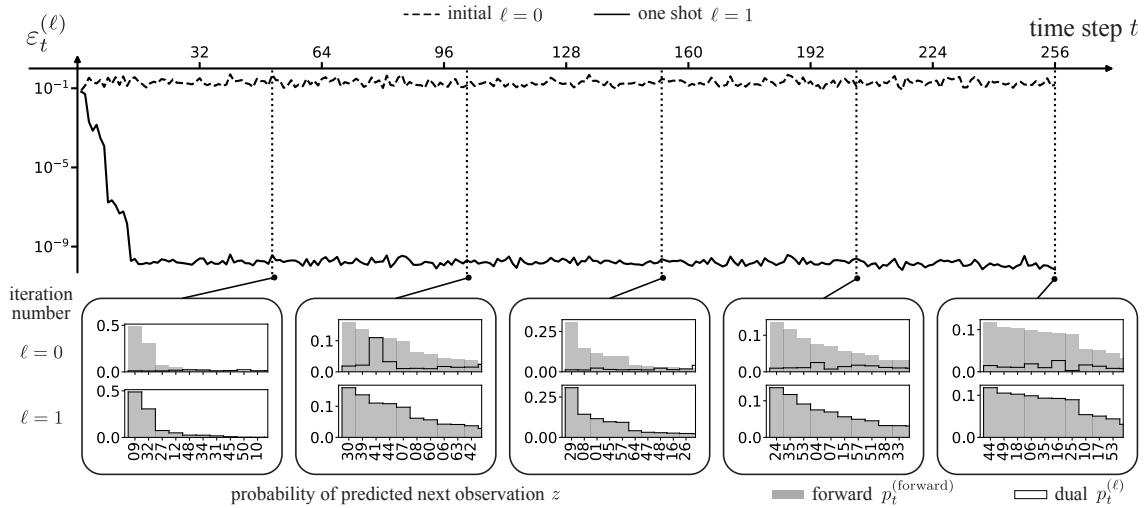


Figure 4: Comparison with the single-shot algorithm. (Top): Time traces of the error $\{\epsilon_t^{(\ell)} : 1 \leq t \leq T\}$ for $\ell = 0, 1$. The dashed line corresponds to the initial error ($\ell = 0$), while the solid line shows the error after one iteration ($\ell = 1$). (Bottom): Top-ten conditional probabilities $\{p_i^{(\ell)}(z_i) : i = 1, \dots, 10\}$ for five representative time points. For each t , these are obtained by sorting the conditional probability vector and selecting the top ten. The gray shading indicates the ground truth (from the nonlinear filter), and the solid line shows the result from the dual filter.

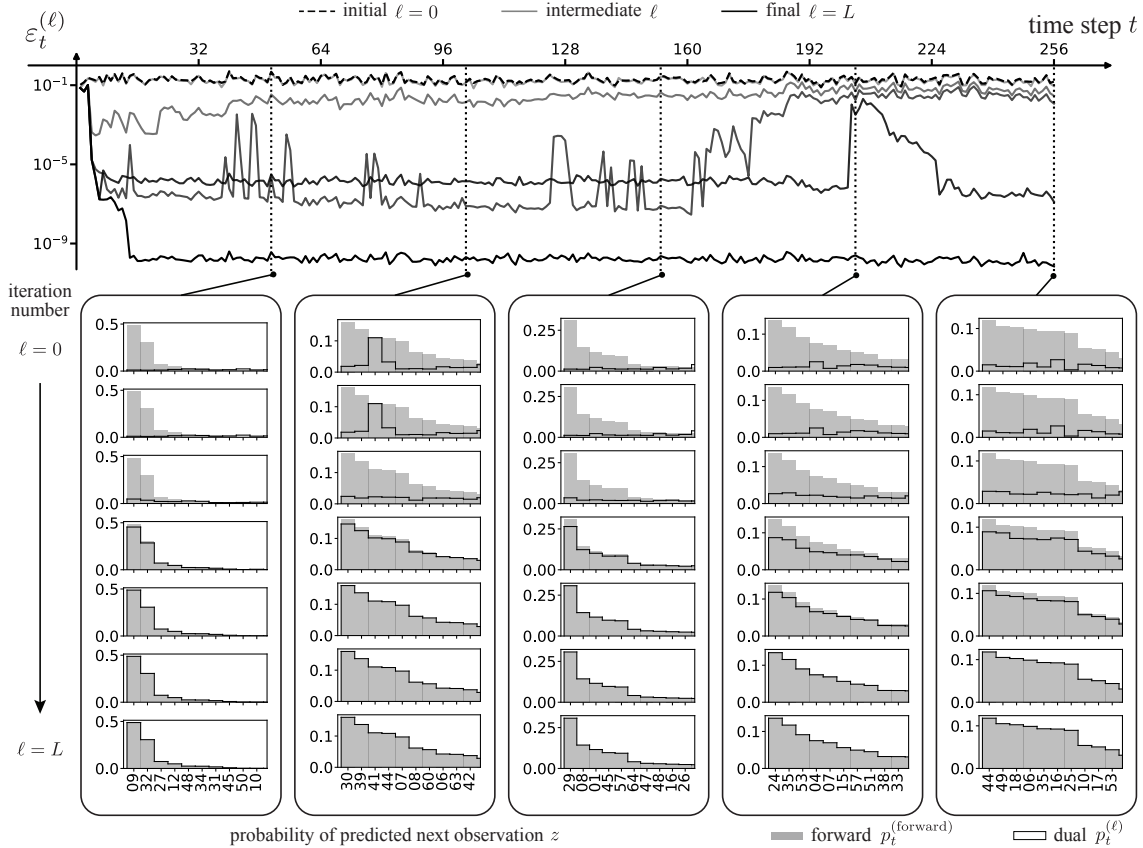


Figure 5: Comparison with the iterative algorithm: (Top): Time traces of the error $\{\varepsilon_t^{(\ell)} : 1 \leq t \leq T\}$ for $\ell = 1, 2, \dots, L$ (with $L = 6$). The dashed line corresponds to the initial error ($\ell = 0$), while the solid lines show the error after subsequent iterations, with darker shades used as ℓ increases. (Bottom): Top-ten conditional probabilities $\{p_t^{(\ell)}(z_i) : i = 1, \dots, 10\}$ for five representative time points. For each t , these are obtained by sorting the conditional probability vector and selecting the top ten. The gray shading indicates the ground truth (from the nonlinear filter), and the solid line shows the result from the dual filter.

5.2 Optimal control input

Representation (1) is helpful for visualizing and understanding the short- and long-term correlations. To illustrate this, Fig. 6 shows the optimal control input for three different values of the homotopy parameter α :

1. For a small value of α such that $|\lambda_2| = 0.3$, the Markovian dynamics mix rapidly. As a result, only the most recent observations contribute meaningfully to prediction at the terminal time T . The control is nonzero only over the most recent few time steps.
2. For $\alpha = 1$, the dynamics are deterministic. In this case, the control is nonzero during the initial phase ($t \leq 5$) when the state is uncertain. At $t = 6$, after the first six observations, the state becomes known (up to numerical precision), and the control input drops to zero (again, up to numerical precision).

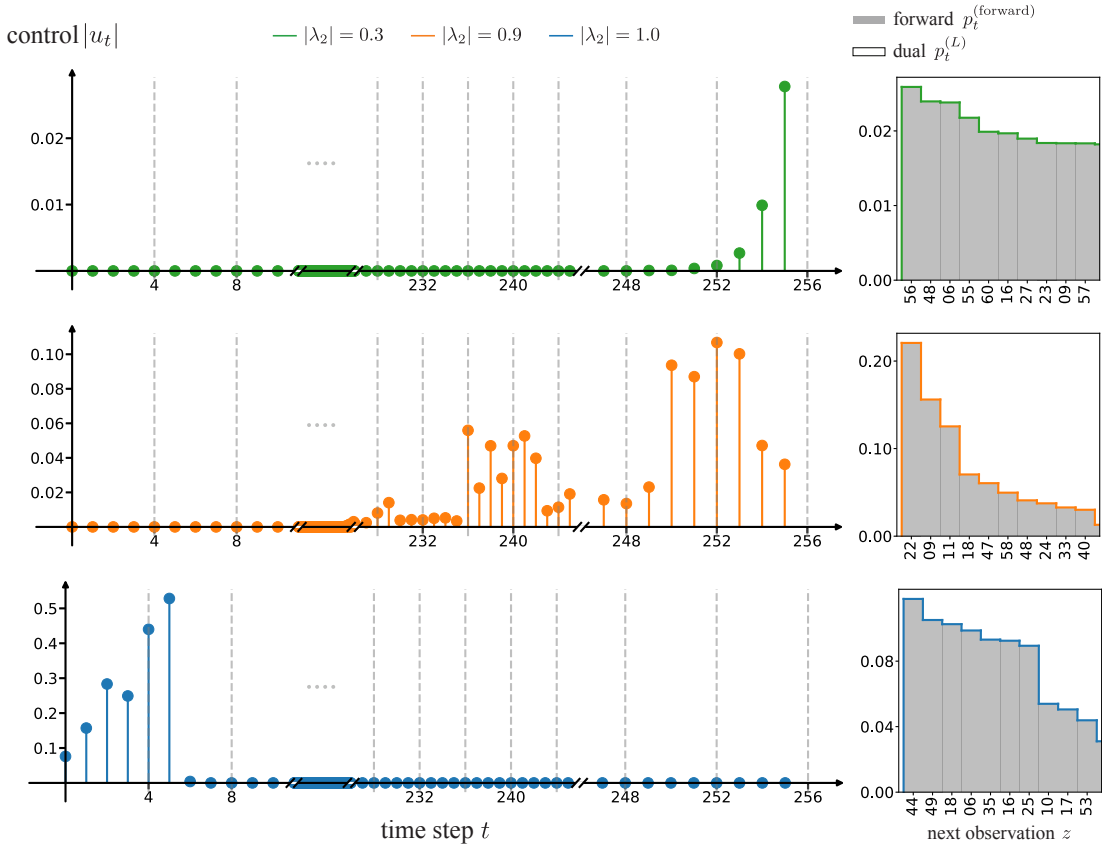


Figure 6: Optimal control inputs as a function of $|\lambda_2|$. (Top): $|\lambda_2| = 0.3$ (green), (Middle): $|\lambda_2| = 0.9$ (orange), (Bottom): $|\lambda_2| = 1.0$ (blue). These three cases correspond to different values of the homotopy parameter α . Note that the x-axis (time t) is plotted on a non-linear scale. The right-hand panels show the top ten conditional probabilities $\{p_T^{(\ell)}(z_i) : i = 1, \dots, 10\}$ at the terminal time $t = T$. These are obtained by sorting the conditional probability vector and selecting the top ten.

3. For an intermediate value of α such that $|\lambda_2| = 0.9$, the control input remains nonzero over an extended time horizon, reflecting the presence of longer-range correlations. Among the three cases, we believe this setting is most representative of the behavior observed in transformer-based predictions.

While Fig. 6 shows the control input for a single sample path of the output, Fig. 7 depicts control inputs computed for ten independent sample paths. For each fixed value of α , ten sample paths of the output sequence are generated. For each sample path, the single-shot dual filter is simulated to compute the corresponding control input.

For $|\lambda_2| = 0.3$, the control inputs are nearly identical across all ten sample paths, suggesting that the predictor behaves approximately linearly. In contrast, for the other two cases, where the spectral gap is smaller, the control inputs exhibit greater variability. Nevertheless, the qualitative structure of the control—such as the time window over which it is nonzero—is consistent across sample paths. This consistency is because of the relatively simple structure of the transition matrix. For a more complicated multi-scale-type choice of the transition matrix A , this is expected to change.

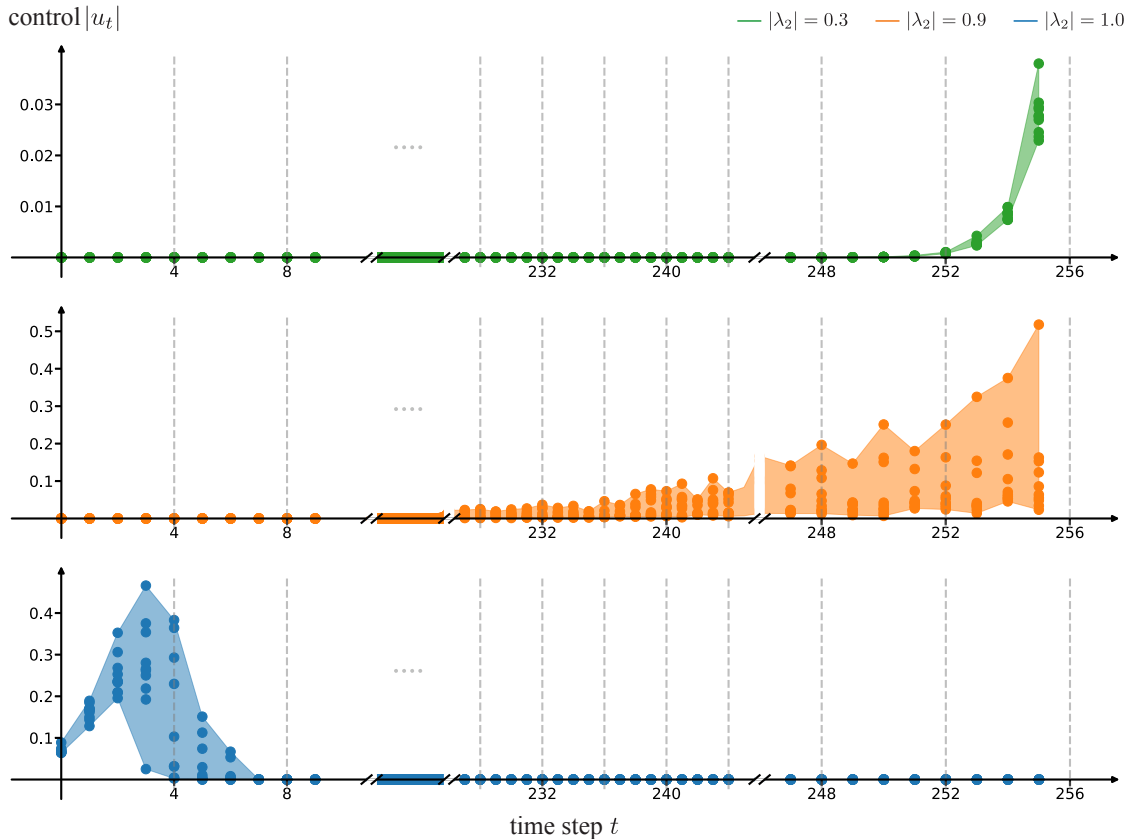


Figure 7: Optimal control inputs across 10 sample paths: (Top): $|\lambda_2| = 0.3$ (green), (Middle): $|\lambda_2| = 0.9$ (orange), (Bottom): $|\lambda_2| = 1.0$ (blue). The shaded region shows the range of control values (minimum to maximum) across the 10 realizations. Note that the scale for the x -axis (denoting time t) is not linear.

5.3 Comparison with transformer

While the scope of numerics is limited to the validation of the dual filter algorithm in model-based settings, a small set of numerical experiments were also carried out using nanoGPT (Karpathy, 2024). For these experiments, nanoGPT is first trained using the data generated from an HMM. Once trained, the model is evaluated for the next-token prediction task. A summary of these numerical evaluations is as follows:

1. For model choices where the prediction p_T is supported on a relatively small subset of the vocabulary \mathbb{O} , the transformer exhibits good performance comparable to the dual filter.
2. For other choices, including for the model discussed as part of Fig. 5, the nanoGPT performance is comparatively poor.

The details are included in Appendix J.

A direct empirical comparison of the dual filter (or a learning variant) against transformer models on general ML tasks (like language modeling) requires the development of a learning framework that is outside the scope of the current foundational paper. Some of these learning-related tasks are planned as part of the future work and briefly described next.

6 Discussion and directions for future work

In this paper, we developed theory and algorithms for a nonlinear predictor based on the representation in (1). We identify two uses of this representation, which motivate two main directions for future research.

1. Analysis: A key outcome of this paper is the fixed-point representation of the conditional measure (posterior) π . The representation invites work on contraction analysis of the mapping $\mathcal{N}^{(\text{dfftr})}$ as well as for the analysis of filter stability.

2. Learning: The objective here is to develop algorithms to learn the layer transformation $\mathcal{N}^{(\text{dfftr})}$. In its basic form, this may be accomplished through learning a parametrized model for (μ, A, C) . There are lessons to be drawn from the reinforcement learning (RL) literature in the setting of partially observed Markov decision processes (POMDPs). In such problems, a key challenge is that the model (μ, A, C) of the hidden Markov process is not known, making it difficult to represent and compute the nonlinear filter (or belief state) directly. To solve this problem, two complementary approaches are commonly considered:

1. A generative model approach, where a parametrized model (for (μ, A, C)) is learned and subsequently used to construct the filter (e.g., using the forward algorithm described in Sec. 1).
2. A history-based approach, where representations are learned directly based on the history—past observations and past actions in the settings of POMDP.

Since the 1990s, empirical evidence suggests that the history-based approach is preferable in RL settings (McCallum, 1996). This has led to the development of several frameworks, namely, predictive state representation (Littman and Sutton, 2001; Rudary and Singh, 2003), which is itself based on the observable operator models (OOM) in un-controlled settings (Jaeger, 2000), and more recently the approximate information state (AIS) (Subramanian et al., 2022; Kao and Subramanian, 2022). It will be of interest to relate (1) to these history-based approaches. The theoretical framework presented in this paper provides a baseline for what an inference architecture can achieve when the data is generated from an HMM. Of course, it will be interesting to extend the framework to a more general class of non-Markovian correlations found in the real-world data. A more fruitful avenue may be to understand the significance of differences, specifically,

- the use of positional encoding to encode the temporal structure in a transformer; and
- the advantages such encodings provide for learning and prediction tasks.

A related goal is the use of the representation (1) for POMDPs. Empirical studies that use transformer architectures for control have appeared in Chen et al. (2021); Zhang et al. (2024); Guo et al. (2024); Ziemann et al. (2024).

For both analysis and learning, the recent paper of Yüksel (2025) is foundational. The paper describes conditions—related to filter stability (van Handel, 2009; Chigansky et al., 2009)—under which purely data-driven approximations are meaningful for control. It is a goal of the ongoing research to better understand the role that these conditions play for the dual filter.

Acknowledgments and Disclosure of Funding

This work is supported in part by the AFOSR award FA9550-23-1-0060 and the NSF award 2336137. Prashant Mehta acknowledges several useful conversations on the topics of transformers and large language models with Dr. Alberto Speranzon. The original research reported in this paper builds upon prior work on duality theory carried out in collaboration with Dr. Jin-Won Kim. These past collaborations are gratefully acknowledged.

Appendix A. Existence proofs

The existence theorems rely on the following proposition from linear algebra.

Proposition 17 *Let $s : \mathbb{O} \rightarrow \mathbb{R}$. Then there exists unique $(\bar{s}, \tilde{s}) \in \mathbb{R} \times \mathbb{R}^m$ such that the following decomposition holds:*

$$s(z) = \bar{s} + \tilde{s}^T e(z), \quad z \in \mathbb{O}.$$

Explicitly,

$$\bar{s} := \frac{1}{m+1} \sum_{z \in \mathbb{O}} s(z), \quad \text{and} \quad \tilde{s}(i) = (s(i) - \bar{s}), \quad i = 1, 2, \dots, m.$$

Proof We have

$$(\bar{s} + \tilde{s}^T e(z)) = \begin{cases} (\bar{s} + (s(z) - \bar{s})) = s(z), & z = 1, 2, \dots, m, \\ (\bar{s} - \tilde{s}^T \mathbf{1}) = s(0), & z = 0, \end{cases}$$

where the last step follows because

$$\tilde{s}^T \mathbf{1} = \sum_{i=1}^m \tilde{s}(i) = \sum_{i=1}^m (s(i) - \bar{s}) = -m\bar{s} + \sum_{i=1}^m s(i),$$

and therefore,

$$\bar{s} - \tilde{s}^T \mathbf{1} = \bar{s} - \left(-m\bar{s} + \sum_{i=1}^m s(i) \right) = (m+1)\bar{s} - \sum_{i=1}^m s(i) = s(0).$$

The decomposition is unique because $\bar{s} + \tilde{s}^T e(z) \equiv 0$ implies

$$\begin{aligned} \bar{s} + \tilde{s}^T e(i) &= \bar{s} + \tilde{s}(i) = 0, \quad i = 1, 2, \dots, m, \\ \bar{s} + \tilde{s}^T e(0) &= \bar{s} - \sum_{i=1}^m \tilde{s}(i) = 0. \end{aligned}$$

Summing the first of these equations over i ,

$$m\bar{s} + \sum_{i=1}^m \tilde{s}(i) = (m+1)\bar{s} = 0,$$

which then also implies $\tilde{s}(i) = -\bar{s} = 0$ for $i = 1, 2, \dots, m$. ■

Example 3 (m=1) Let $s : \{0, 1\} \rightarrow \mathbb{R}$. Denote $s^+ := s(1)$ and $s^- := s(0)$. Then

$$s(z) = \bar{s} + \tilde{s}e(z), \quad z \in \{0, 1\},$$

where $\bar{s} := \frac{1}{2}(s^+ + s^-)$ and $\tilde{s} := \frac{1}{2}(s^+ - s^-)$ (recall $e(1) = 1$ and $e(0) = -1$).

Remark 18 There is nothing special about the choice of $\{e(1), e(2), \dots, e(m)\}$, chosen in this paper to be the canonical basis. One could instead choose these vectors to be any basis of \mathbb{R}^m , and set $e(0) = -e(1) - e(2) - \dots - e(m)$ as before. In Fukasawa et al. (2025), such a structure is referred to as a lattice. See (Cohen and Elliott, 2010) for a general theory of BSΔE.

A.1 Well-posedness of representation (1) (Proof of Prop. 6)

Proof [of Prop. 6] We begin by proving a result where the representation is shown to hold for *any* $S_T \in \mathcal{Z}_T$. From Doob-Dynkin lemma, there is a deterministic function $s : \mathbb{O}^T \rightarrow \mathbb{R}$ such that

$$S_T = s(Z_1, \dots, Z_{T-1}, Z_T).$$

Set

$$S(z) := s(Z_1, \dots, Z_{T-1}, z), \quad z \in \mathbb{O}.$$

From Prop. 17,

$$S_T = S(Z_T) = S_{T-1} - (U_{T-1})^\top e(Z_T),$$

where

$$S_{T-1} = \frac{1}{m+1} \sum_{z \in \mathbb{O}} S(z), \quad U_{T-1}(i) := -(S(i) - S_{T-1}), \quad i = 1, 2, \dots, m.$$

Uniqueness is from the uniqueness of the decomposition. The proof is completed through induction by repeating the procedure for $S_{T-1} \in \mathcal{Z}_{T-1}$.

A direct application of the above result to justify the representation (1) for $\pi_T(F)$ is complicated by a subtle issue: The conditional expectation $\pi_T(F)$ is meaningfully defined only for sample paths $Z = z$ with $P([Z = z]) > 0$. Note here that because $|\mathbb{O}| = m + 1$ and T are both finite, there are only finitely many—specifically $(m + 1)^T$ —sample paths. Thus, $P([Z = z])$ is a well-defined object for each sample path, although it may be zero depending on the HMM parameters (μ, A, C) .

There are two ways to address this issue:

1. Assume $\underline{c} := \min\{C(x, z) : x \in \mathbb{S}, z \in \mathbb{O}\} > 0$. Then $P([Z = z]) \geq \underline{c}^T > 0$ for all $z \in \mathbb{O}^T$, and the existence of a unique U follows directly from the earlier result.
2. Adopt the convention $\frac{0}{0} = 0$ to define (or extend) the conditional measure for sample paths $Z = z$ with $P([Z = z]) = 0$. Then again, a particular selection of U follows from the above result.

In the second case, however, there may be other choices of U such that the representation (1) holds: Any two choices will yield a representation that coincides on the set $\{z \in \mathbb{O}^T : P(Z = z) > 0\}$ but may differ on the set $\{z \in \mathbb{O}^T : P(Z = z) = 0\}$. ■

Remark 19 (Extension to non-Markovian settings) *To prove Prop. 6, we did not make use of the Markov property of the latent process X . While the focus of the present paper is on the HMM, the representation (1) holds also in more general non-Markovian settings. The Markovian assumption is introduced solely to obtain an explicit formula for U .*

Example 4 (m=1) *Set $S_T^+ = s(Z_1, \dots, Z_{T-1}, 1)$ and $S_T^- = s(Z_1, \dots, Z_{T-1}, 0)$. Then $S_T^+, S_T^- \in \mathcal{Z}_{T-1}$ and*

$$S_T = S_{T-1} - U_{T-1}e(Z_T),$$

where $S_{T-1} = \frac{1}{2}(S_T^+ + S_T^-)$ and $U_{T-1} = -\frac{1}{2}(S_T^+ - S_T^-)$.

A.2 Well-posedness of BSΔE (2) (Proof of Prop. 8)

Proof [of Prop. 8] Fix $x \in \mathbb{S}$. Then at time $t = T$, the BSΔE is

$$(AF)(x) = Y_{T-1}(x) - c^\top(x)(U_{T-1} + V_{T-1}(x)) + (V_{T-1}(x))^\top e(Z_T), \quad x \in \mathbb{S}.$$

Because A is deterministic $(AF)(x) \in \mathcal{Z}_T$ and therefore there is a deterministic function $s : \mathbb{O}^T \times \mathbb{S} \rightarrow \mathbb{R}$ such that

$$(AF)(x) = s(Z_1, \dots, Z_{T-1}, Z_T; x), \quad x \in \mathbb{S}.$$

Set

$$S(z; x) := s(Z_1, \dots, Z_{T-1}, z; x), \quad z \in \mathbb{O}, \quad x \in \mathbb{S}.$$

From Prop. 17, there exists unique $\bar{S}_{T-1}(x), \tilde{S}_{T-1}(x) \in \mathcal{Z}_{T-1}$ such that

$$(AF)(x) = S(Z_T; x) = \bar{S}_{T-1}(x) + (\tilde{S}_{T-1}(x))^\top e(Z_T), \quad x \in \mathbb{S}.$$

Set

$$\begin{aligned} V_{T-1}(x) &= \tilde{S}_{T-1}(x), \quad x \in \mathbb{S}, \\ Y_{T-1}(x) &= \bar{S}_{T-1}(x) + c^\top(x)(U_{T-1} + V_{T-1}(x)), \quad x \in \mathbb{S}. \end{aligned}$$

Uniqueness follows from the uniqueness of decomposition. Because $Y_{T-1} \in \mathcal{Z}_{T-1}$, the proof is completed through induction. ■

Example 5 (m=1) *For each $x \in \mathbb{S}$, set $S_T^+(x) = s(Z_1, \dots, Z_{T-1}, 1; x)$ and $S_T^-(x) = s(Z_1, \dots, Z_{T-1}, 0; x)$. Then $S_T^+(x), S_T^-(x) \in \mathcal{Z}_{T-1}$ and*

$$\begin{aligned} V_{T-1}(x) &= \frac{1}{2}(S_T^+(x) - S_T^-(x)), \quad x \in \mathbb{S}, \\ Y_{T-1}(x) &= \frac{1}{2}(S_T^+(x) + S_T^-(x)) + c(x)(U_{T-1} + V_{T-1}(x)), \quad x \in \mathbb{S}. \end{aligned}$$

Appendix B. Proof of Prop. 7

Based on the graphical model for the HMM (see Fig. 1), $X_{t+1} \perp\!\!\!\perp Z_{t+1} \mid \mathcal{F}_t$. Therefore,

$$\mathbb{E}(B_{t+1}(f) \mid \mathcal{F}_t \vee \mathcal{Z}_{t+1}) = \mathbb{E}(f(X_{t+1}) \mid \mathcal{F}_t \vee \mathcal{Z}_{t+1}) - (Af)(X_t) = \mathbb{E}(f(X_{t+1}) \mid \mathcal{F}_t) - (Af)(X_t) = 0,$$

and

$$\begin{aligned} \mathbb{E}(|B_{t+1}(f)|^2 | \mathcal{F}_t \vee \mathcal{Z}_{t+1}) &= \mathbb{E}(|f(X_{t+1}) - (Af)(X_t)|^2 | \mathcal{F}_t) \\ &= \mathbb{E}(|f(X_{t+1})|^2 | \mathcal{F}_t) - |(Af)(X_t)|^2 = (\Gamma f)(X_t), \end{aligned}$$

for $t = 0, 1, 2, \dots, T-1$. This completes the proof for the two formulae related to the process B .

Express the vector-valued functions $e : \mathbb{O} \rightarrow \mathbb{R}^m$ as

$$e(z) = \begin{bmatrix} g_1(z) \\ g_2(z) \\ \vdots \\ g_m(z) \end{bmatrix}_{m \times 1}, \quad \text{where } g_i(z) = \begin{cases} -1, & z = 0 \\ 1, & z = i, \quad i = 1, 2, \dots, m, \\ 0, & \text{o.w.} \end{cases}$$

where note

$$(Cg_i)(x) = c(x), \quad x \in \mathbb{S}, \quad i = 1, 2, \dots, m.$$

Therefore,

$$W_{t+1}(i) = g_i(Z_{t+1}) - (Cg_i)(X_t), \quad t = 0, 1, 2, \dots, T-1, \quad i = 1, 2, \dots, m,$$

and because $\mathbb{P}(Z_{t+1} = z | X_t = x) = C(x, z)$ for $x \in \mathbb{S}$ and $z \in \mathbb{O}$,

$$\mathbb{E}(W_{t+1}(i) | \mathcal{F}_t) = \sum_{z \in \mathbb{O}} C(X_t, z) g_i(z) - (Cg_i)(X_t) = 0, \quad t = 0, 1, 2, \dots, T-1, \quad i = 1, 2, \dots, m.$$

This shows that W is a martingale increment process. It remains to derive the formula for the $m \times m$ matrix R . In order to determine the (i, j) -entry of the matrix R , we consider $\mathbb{E}(W_{t+1}(i)W_{t+1}(j) | \mathcal{F}_t)$. From the definition of W ,

$$\begin{aligned} g_i(Z_{t+1}) &= (Cg_i)(X_t) + W_{t+1}(i), \quad t = 0, 1, 2, \dots, T-1, \quad i = 1, 2, \dots, m, \\ g_j(Z_{t+1}) &= (Cg_j)(X_t) + W_{t+1}(j), \quad t = 0, 1, 2, \dots, T-1, \quad j = 1, 2, \dots, m. \end{aligned}$$

Then because W is a martingale increment process,

$$\begin{aligned} \mathbb{E}(g_i(Z_{t+1})g_j(Z_{t+1}) | \mathcal{F}_t) &= (Cg_i)(X_t)(Cg_j)(X_t) + \mathbb{E}(W_{t+1}(i)W_{t+1}(j) | \mathcal{F}_t) \\ &= c(X_t)c(X_t) + \mathbb{E}(W_{t+1}(i)W_{t+1}(j) | \mathcal{F}_t). \end{aligned}$$

Now, the left-hand side

$$\begin{aligned} \mathbb{E}(g_i(Z_{t+1})g_j(Z_{t+1}) | \mathcal{F}_t) &= \sum_{z \in \mathbb{O}} g_i(z)g_j(z)C(X_t, z) \\ &= g_i(0)g_j(0)C(X_t, 0) + \sum_{z=1}^m g_i(z)g_j(z)C(X_t, z) \\ &= C(X_t, 0) + \delta_{ij}C(X_t, i), \end{aligned}$$

where $\{\delta_{ij} : 1 \leq i \leq m, 1 \leq j \leq m\}$ is the Kronecker δ . Combining,

$$\mathbb{E}(W_{t+1}(i)W_{t+1}(j) | \mathcal{F}_t) = C(X_t, 0) + \delta_{ij}C(X_t, i) - c(X_t)c(X_t), \quad 0 \leq t \leq T-1, \quad 1 \leq i, j \leq m.$$

Expressed in the matrix form,

$$\mathbb{E}(W_{t+1}W_{t+1}^\top | \mathcal{F}_t) = R(X_t), \quad 0 \leq t \leq T-1.$$

The meaning of $R(x)$ is as follows:

$$u^\top R(x)u = C(x,0)(-1^\top u)^2 + \sum_{i=1}^m C(x,i)(u(i))^2 - \left(C(x,0)(-1^\top u) + \sum_{i=1}^m C(x,i)u(i) \right)^2, \quad x \in \mathbb{S}, \quad u \in \mathbb{R}^m,$$

where $1^\top u = \sum_{i=1}^m u(i)$. Note that for each fixed $x \in \mathbb{S}$, $C(x, \cdot)$ is a $1 \times m$ probability vector. Therefore, $u^\top R(x)u$ is the variance of $\begin{bmatrix} (-1^\top u) \\ u \end{bmatrix} \in \mathbb{R}^{m+1}$, with respect to the probability vector $C(x, \cdot)$.

Appendix C. Proof of Thm. 9 (Duality principle)

We prove a result for a more general class of estimators of the form

$$S_T = c_0 - \sum_{t=0}^{T-1} U_t^\top e(Z_{t+1}),$$

where $U \in \mathcal{U}$ and c_0 is a deterministic constant (note that in the statement of Thm. 9, $c_0 = \mu(Y_0)$). For any such estimator, we show

$$\mathbb{E}(|F(X_T) - S_T|^2) = J_T(U; F) + (\mu(Y_0) - c_0)^2. \quad (11)$$

This more general formula is useful for another proof (see Appendix D).

For the HMM, we have defined two martingale increment processes (see Sec. 2.1):

$$\begin{aligned} B_{t+1}(f) &= f(X_{t+1}) - (Af)(X_t), \quad 0 \leq t \leq T-1, \\ W_{t+1} &= e(Z_{t+1}) - c(X_t), \quad 0 \leq t \leq T-1. \end{aligned}$$

Taking $f = Y_{t+1}$,

$$B_{t+1}(Y_{t+1}) = Y_{t+1}(X_{t+1}) - (AY_{t+1})(X_t), \quad 0 \leq t \leq T-1.$$

Since Y solves BSΔE (2),

$$(AY_{t+1})(x) = Y_t(x) - c^\top(x)(U_t + V_t(x)) + V_t^\top(x)e(Z_{t+1}), \quad \forall x \in \mathbb{S}, \quad 0 \leq t \leq T-1,$$

and therefore at $x = X_t$,

$$(AY_{t+1})(X_t) = Y_t(X_t) - c^\top(X_t)(U_t + V_t(X_t)) + V_t^\top(X_t)e(Z_{t+1}), \quad 0 \leq t \leq T-1.$$

Because $W_{t+1} = e(Z_{t+1}) - c(X_t)$, we have

$$\begin{aligned} c^\top(X_t)U_t &= U_t^\top e(Z_{t+1}) - U_t^\top W_{t+1}, \quad 0 \leq t \leq T-1, \\ c^\top(X_t)V_t(X_t) &= V_t^\top(X_t)e(Z_{t+1}) - V_t^\top(X_t)W_{t+1}, \quad 0 \leq t \leq T-1, \end{aligned}$$

and thus,

$$(AY_{t+1})(X_t) = Y_t(X_t) - U_t^\top e(Z_{t+1}) + (U_t + V_t(X_t))^\top W_{t+1}, \quad 0 \leq t \leq T-1.$$

Therefore,

$$\begin{aligned} Y_{t+1}(X_{t+1}) &= (AY_{t+1})(X_t) + B_{t+1}(Y_{t+1}), \quad 0 \leq t \leq T-1 \\ &= Y_t(X_t) - U_t^\top e(Z_{t+1}) + (U_t + V_t(X_t))^\top W_{t+1} + B_{t+1}(Y_{t+1}), \quad 0 \leq t \leq T-1. \end{aligned}$$

Summing over $t = 0, 1, 2, \dots, T-1$, using the form of the estimator S_T and because $Y_T = F$,

$$F(X_T) - S_T = (Y_0(X_0) - c_0) + \sum_{t=0}^{T-1} N_{t+1},$$

where

$$N_{t+1} := (U_t + V_t(X_t))^\top W_{t+1} + B_{t+1}(Y_{t+1}), \quad t = 0, 1, \dots, T-1,$$

is a sum of two martingale increment processes.

Formula (11) is obtained from squaring both sides and taking expectations. Formulae for the non-zero terms are as follows (for this purpose, denote $\mathcal{G}_t := \mathcal{F}_{t-1} \vee \mathcal{Z}_t$ for $t = 1, 2, \dots, T$):

$$\begin{aligned} \mathbb{E}(|Y_0(X_0) - \mu(Y_0)|^2) &= \text{var}(Y_0(X_0)), \\ \mathbb{E}(((U_t^\top + V_t^\top(X_t))W_{t+1})^2) &= \mathbb{E}((U_t^\top + V_t^\top(X_t))\mathbb{E}(W_{t+1}W_{t+1}^\top|\mathcal{F}_t)(U_t + V_t(X_t))), \\ &= \mathbb{E}((U_t^\top + V_t^\top(X_t))R(X_t)(U_t + V_t(X_t))) \\ \mathbb{E}((B_{t+1}(Y_{t+1}))^2) &= \mathbb{E}(\mathbb{E}((B_{t+1}(Y_{t+1}))^2|\mathcal{G}_{t+1})) = \mathbb{E}((\Gamma Y_{t+1})(X_t)). \end{aligned}$$

The cross-terms are zero because

$$\begin{aligned} \mathbb{E}((Y_0(X_0) - \mu(Y_0))(U_t^\top + V_t^\top(X_t))\mathbb{E}(W_{t+1}|\mathcal{F}_t)) &= 0, \\ \mathbb{E}((Y_0(X_0) - \mu(Y_0))\mathbb{E}(B_{t+1}(Y_{t+1})|\mathcal{G}_{t+1})) &= 0, \\ \mathbb{E}((U_t^\top + V_t^\top(X_t))W_{t+1}\mathbb{E}(B_{t+1}(Y_{t+1})|\mathcal{G}_{t+1})) &= 0, \end{aligned}$$

and for $\tau > t$,

$$\begin{aligned} \mathbb{E}((U_t^\top + V_t^\top(X_t))W_{t+1}(U_\tau + V_\tau(X_\tau))\mathbb{E}(W_{\tau+1}|\mathcal{F}_\tau)) &= 0, \\ \mathbb{E}(B_{t+1}(Y_{t+1})\mathbb{E}((U_\tau^\top + V_\tau^\top(X_\tau))W_{\tau+1}|\mathcal{F}_\tau)) &= 0, \\ \mathbb{E}(B_{t+1}(Y_{t+1})\mathbb{E}(B_{\tau+1}(Y_{\tau+1})|\mathcal{G}_{\tau+1})) &= 0, \\ \mathbb{E}((U_t^\top + V_t^\top(X_t))W_{t+1}\mathbb{E}(B_{\tau+1}(Y_{\tau+1})|\mathcal{G}_{\tau+1})) &= 0. \end{aligned}$$

Appendix D. Proof of Prop. 10

From the existence result described in Prop. 6, there exists a $c^* \in \mathbb{R}$ and $U^* = \{U_t^* : 0 \leq t \leq T-1\} \in \mathcal{U}$ such that

$$\pi_T(F) = c^* - \sum_{t=0}^{T-1} (U_t^*)^\top e(Z_{t+1}), \quad \text{P-a.s.}$$

From the duality principle (see the formula (11) shown in Appendix C),

$$\mathbb{E}(|F(X_T) - \pi_T(F)|^2) = J_T(U^*; F) + (c^* - \mu(Y_0^*))^2,$$

where Y_0^* is obtained from solving the BSΔE (2) with control $U = U^*$.

We show that U^* is an optimal control. Suppose there exists a $\tilde{U} \in \mathcal{U}$ such that

$$J_T(U^*; F) \geq J_T(\tilde{U}; F).$$

Then set $\tilde{S} = \mu(\tilde{Y}_0) - \sum_{t=0}^{T-1} \tilde{U}_t^\top e(Z_{t+1})$ where \tilde{Y}_0 is obtained from solving the BSDE (2) with control $U = \tilde{U}$. Then using the duality principle,

$$J_T(\tilde{U}; F) = \mathbb{E}(|F(X_T) - \tilde{S}|^2) \geq \mathbb{E}(|F(X_T) - \pi_T(F)|^2),$$

where the inequality is from the MMSE property of the conditional expectation.

Combining,

$$\begin{aligned} \mathbb{E}(|F(X_T) - \pi_T(F)|^2) &= J_T(U^*; F) + (c^* - \mu(Y_0^*))^2 \\ &\geq J_T(\tilde{U}; F) + (c^* - \mu(Y_0^*))^2 \\ &= \mathbb{E}(|F(X_T) - \tilde{S}|^2) + (c^* - \mu(Y_0^*))^2 \\ &\geq \mathbb{E}(|F(X_T) - \pi_T(F)|^2) + (c^* - \mu(Y_0^*))^2. \end{aligned}$$

It then follows that $c^* = \mu(Y_0^*)$ and all the inequalities are in fact equalities. In particular,

$$J_T(\tilde{U}; F) = J_T(U^*; F) = \mathbb{E}(|F(X_T) - \pi_T(F)|^2) = \text{MMSE}.$$

This proves existence—both \tilde{U} and U^* are optimal controls that attain the optimal value given by MMSE. Moreover,

$$\mathbb{E}(|F(X_T) - \tilde{S}|^2) = \mathbb{E}(|F(X_T) - \pi_T(F)|^2) \implies \tilde{S} = \pi_T(F), \quad \text{P-a.s.}$$

because of the uniqueness property of the conditional expectation.

Remark 20 *To conclude uniqueness (that is, $U^* = \tilde{U}$, P-a.s.) requires additional assumption on the model. For example, a sufficient condition for the same is to assume $C(x, z) > 0$ for all $x \in \mathbb{S}$ and $z \in \mathbb{O}$. Then the proof of Prop. 6 shows that U^* is unique (see Appendix A.1). Because U^* is an optimal control input, it follows that the optimal control input is unique.*

Appendix E. Proof of Thm. 11

The formula for the optimal control is easiest to see from the consideration of the OCP (3) for $T = 1$.

E.1 Formula for the optimal control for $T = 1$

With $T = 1$, the OCP (3) is

$$\begin{aligned} \min_{U_0 \in \mathbb{R}^m} \quad & J_1(U_0; F) = \mu(Y_0^2) - \mu(Y_0)^2 + \mathbb{E}(l(F, V_0, U_0; X_0)), \\ \text{subject to} \quad & Y_0(x) = (AF)(x) + c^\top(x)(U_0 + V_0(x)) - V_0^\top(x)e(Z_1), \quad x \in \mathbb{S}. \end{aligned}$$

Because $F(x) \in \mathcal{Z}_1$, there exists the deterministic $s: \mathbb{S} \times \mathbb{O} \rightarrow \mathbb{R}$ such that

$$F(x) = s(x, Z_1), \quad x \in \mathbb{S}.$$

Define

$$f(x) := \frac{1}{m+1} \sum_{z \in \mathbb{O}} s(x, z), \quad \tilde{s}_i(x) := s(x, i) - f(x), \quad i = 1, 2, \dots, m, \quad x \in \mathbb{S}.$$

Then using Prop. 17,

$$s(x, z) = f(x) + \tilde{s}(x)e(z), \quad z \in \mathbb{O}, \quad x \in \mathbb{S},$$

where $\tilde{s}(\cdot) = [\tilde{s}_1(\cdot) \quad \tilde{s}_2(\cdot) \quad \dots \quad \tilde{s}_m(\cdot)]_{d \times m}$. Therefore,

$$F(x) = s(x, Z_1) = f(x) + \tilde{s}(x)e(Z_1), \quad x \in \mathbb{S}.$$

Based on the decomposition above,

$$\begin{aligned} (AF)(x) &= (Af)(x) + (A\tilde{s})(x)e(Z_1), \quad x \in \mathbb{S}, \\ &= Y_0(x) - c^T(x)(U_0 + V_0(x)) + V_0^T(x)e(Z_1), \quad x \in \mathbb{S}, \end{aligned}$$

which gives

$$\begin{aligned} V_0(x) &= (A\tilde{s})^T(x), \quad x \in \mathbb{S}, \\ Y_0(x) &= (Af)(x) + c^T(x)(U_0 + V_0(x)), \quad x \in \mathbb{S}. \end{aligned}$$

Based on this, the OCP reduces to a standard (deterministic) linear quadratic (LQ) problem

$$\min_{U_0 \in \mathbb{R}^m} J_1(U_0; F) = \mu(Y_0^2) - \mu(Y_0)^2 + \sum_x \mu(x)(U_0 + V_0(x))^T R(x)(U_0 + V_0(x)) + E(\Gamma F(X_0)),$$

$$\text{subject to } Y_0(x) = (Af)(x) + c^T(x)(U_0 + V_0(x)), \quad x \in \mathbb{S}.$$

where note $E(\Gamma F(X_0))$ is not affected by the control U_0 . The LQ problem is readily solved to obtain the formula for the optimal control,

$$U_0^{(\text{opt})} = \phi(Y_0^{(\text{opt})}, V_0; \mu),$$

where

$$Y_0^{(\text{opt})}(x) = (Af)(x) + c^T(x)(U_0^{(\text{opt})} + V_0(x)), \quad x \in \mathbb{S}.$$

Let $U_0 = U_0^{(\text{opt})} + \tilde{U}_0$ then

$$Y_0(x) = Y_0^{(\text{opt})}(x) + c^T(x)\tilde{U}_0, \quad x \in \mathbb{S},$$

A standard completion-of-square argument is used to show that

$$\begin{aligned} J_1(U_0; F) &= J_1(U_0^{(\text{opt})}; F) + \mu((c^T \tilde{U}_0)^2) - \mu(c^T \tilde{U}_0)^2 + \sum_x \mu(x) \tilde{U}_0^T R(x) \tilde{U}_0 \\ &= J_1(U_0^{(\text{opt})}; F) + \langle \tilde{U}_0, \tilde{U}_0 \rangle_{p_0}, \end{aligned}$$

where $p_0 = \mu(C)$. Because the calculations are entirely identical also for the general case, these are included in Sec. E.3 at the end of this proof.

From Prop. 10,

$$J_1(U_0^{(\text{opt})}; F) = \text{MMSE} = E(|F(X_1) - \pi_1(F)|^2) = E(\pi_1(F^2) - \pi_1(F)^2),$$

where the last equality is from the use of the tower property. Summarizing,

$$J_1(U_0; F) = E(\pi_1(F^2) - \pi_1(F)^2) + \langle U_0 - U_0^{(\text{opt})}, U_0 - U_0^{(\text{opt})} \rangle_{p_0}. \quad (12)$$

E.2 Proof of Thm. 11

Notation: For a function $f \in \mathbb{R}^d$, and $t \in \mathbb{T}$, denote $\mathcal{V}_t(f) := \pi_t(f^2) - \pi_t(f)^2$. Note $\mathcal{V}_t(f)$ represents the conditional variance of the random variable $f(X_t)$ because $\mathcal{V}_t(f) = \mathbb{E}(|f(X_t) - \pi_t(f)|^2 | \mathcal{Z}_t)$.

Proof [of Thm. 11] Define

$$\begin{aligned} J_1(U_0; Y_1) &:= \mu(Y_0^2) - \mu(Y_0)^2 + \mathbb{E}(l(Y_1, V_0, U_0; X_0)), \\ J_{t+1}(U_0, \dots, U_t; Y_{t+1}) &:= J_t(U_0, \dots, U_{t-1}; Y_t) + \mathbb{E}(l(Y_{t+1}, V_t, U_t; X_t)), \quad t = 1, 2, \dots, T-1. \end{aligned}$$

Note that at the terminal time, this gives the optimal control objective.

The proof of (4b) is by induction based on essentially repeating the calculations described for $T = 1$ in the preceding subsection. Suppose it has already been shown that

$$J_t(U_0, \dots, U_{t-1}; Y_t) = \mathbb{E} \left(\sum_{s=0}^{t-1} \langle \tilde{U}_s, \tilde{U}_s \rangle_{p_s} \right) + \mathbb{E}(\mathcal{V}_t(Y_t)).$$

Our task is to show that

$$J_{t+1}(U_0, \dots, U_t; Y_{t+1}) = \mathbb{E} \left(\sum_{s=0}^t \langle \tilde{U}_s, \tilde{U}_s \rangle_{p_s} \right) + \mathbb{E}(\mathcal{V}_{t+1}(Y_{t+1})),$$

where $\tilde{U}_s = U_s - U_s^{(\text{opt})}$ for $0 \leq s \leq t$. At the terminal time, this is the desired formula (4b).

The base case ($t = 1$) is proved in (12). Using the induction hypothesis, we have

$$\begin{aligned} J_{t+1}(U_0, \dots, U_t; Y_{t+1}) &= J_t(U_0, \dots, U_{t-1}; Y_t) + \mathbb{E}(l(Y_{t+1}, V_t, U_t; X_t)) \\ &= \mathbb{E} \left(\sum_{s=0}^{t-1} \langle \tilde{U}_s, \tilde{U}_s \rangle_{p_s} \right) + \mathbb{E}(\mathcal{V}_t(Y_t)) + \mathbb{E}(l(Y_{t+1}, V_t, U_t; X_t)) \end{aligned}$$

Now,

$$\mathbb{E}(\langle \mathcal{V}_t(Y_t) + l(Y_{t+1}, V_t, U_t; X_t) \rangle | \mathcal{Z}_t) = \mathcal{V}_t(Y_t) + \sum_{x \in \mathbb{S}} \pi_t(x) (U_t + V_t(x))^T R(x) (U_t + V_t(x)) + \pi_t(\Gamma Y_{t+1}),$$

where the $(Y_t, V_t, U_t) \in \mathcal{Z}_t$ are related to $Y_{t+1} \in \mathcal{Z}_{t+1}$ via the BSΔE,

$$Y_t(x) = (AY_{t+1})(x) + c^T(x)(U_t + V_t(x)) - V_t^T(x)e(Z_{t+1}), \quad x \in \mathbb{S}.$$

From the theory for BSΔE described in Appendix A.2, for any given $Y_{t+1} \in \mathcal{Z}_{t+1}$, there exists a unique such $V_t \in \mathcal{Z}_t$ such that above holds. Set

$$U_t^{(\text{opt})} = \phi(Y_t^{(\text{opt})}, V_t; \pi_t),$$

where

$$Y_t^{(\text{opt})}(x) = (AY_{t+1})(x) + c^T(x)(U_t^{(\text{opt})} + V_t(x)) - V_t^T(x)e(Z_{t+1}), \quad x \in \mathbb{S}.$$

Let $U_t = U_t^{(\text{opt})} + \tilde{U}_t$ then

$$Y_t(x) = Y_t^{(\text{opt})}(x) + c^T(x)\tilde{U}_t, \quad x \in \mathbb{S},$$

A completion-of-square argument then gives (the calculations for the same are included in Sec. E.3 at the end of this proof),

$$\begin{aligned} \mathcal{V}_t(Y_t) + \sum_{x \in \mathbb{S}} \pi_t(x) (U_t + V_t(x))^T R(x) (U_t + V_t(x)) \\ = \langle \tilde{U}_t, \tilde{U}_t \rangle_{p_t} + \mathcal{V}_t(Y_t^{(\text{opt})}) + \sum_{x \in \mathbb{S}} \pi_t(x) (U_t^{(\text{opt})} + V_t(x))^T R(x) (U_t^{(\text{opt})} + V_t(x)), \end{aligned}$$

and thus, upon adding $\pi_t(\Gamma Y_{t+1})$ to both sides,

$$\mathcal{V}_t(Y_t) + \mathbb{E}(l(Y_{t+1}, V_t, U_t; X_t) | \mathcal{Z}_t) = \langle \tilde{U}_t, \tilde{U}_t \rangle_{p_t} + \mathcal{V}_t(Y_t^{(\text{opt})}) + \mathbb{E}(l(Y_{t+1}, V_t, U_t^{(\text{opt})}; X_t) | \mathcal{Z}_t).$$

Therefore,

$$\begin{aligned} J_{t+1}(U_0, \dots, U_t; Y_{t+1}) &= J_t(U_0, \dots, U_{t-1}; Y_t) + \mathbb{E}(l(Y_{t+1}, V_t, U_t; X_t)) \\ &= \mathbb{E}\left(\sum_{s=0}^{t-1} \langle \tilde{U}_s, \tilde{U}_s \rangle_{p_s}\right) + \mathbb{E}(\mathcal{V}_t(Y_t)) + \mathbb{E}(l(Y_{t+1}, V_t, U_t; X_t)) \\ &= \mathbb{E}\left(\sum_{s=0}^t \langle \tilde{U}_s, \tilde{U}_s \rangle_{p_s}\right) + \mathbb{E}(\mathcal{V}_t(Y_t^{(\text{opt})})) + \mathbb{E}(l(Y_{t+1}, V_t, U_t^{(\text{opt})}; X_t)). \end{aligned}$$

From Prop. 10,

$$J_{t+1}(U_0^{(\text{opt})}, \dots, U_t^{(\text{opt})}; Y_{t+1}) = \mathbb{E}(\mathcal{V}_{t+1}(Y_{t+1})),$$

and we have established the induction formula for $t+1$. Also from Prop. 10,

$$\pi_{t+1}(Y_{t+1}) = \mu(Y_0^{(\text{opt})}) - \sum_{s=0}^t (U_s^{(\text{opt})})^T e(Z_{s+1}),$$

which proves (4c). ■

E.3 Details of the completion-of-square calculation

Let $U_t = U_t^{(\text{opt})} + \tilde{U}_t$ and $Y_t = Y_t^{(\text{opt})} + \tilde{Y}_t$ where $\tilde{Y}_t(x) = c^T(x) \tilde{U}_t$. Then

$$\begin{aligned} \mathcal{V}_t(Y_t) + \sum_{x \in \mathbb{S}} \pi_t(x) (U_t + V_t(x))^T R(x) (U_t + V_t(x)) &= \left(\mathcal{V}_t(\tilde{Y}_t) + \sum_{x \in \mathbb{S}} \pi_t(x) (\tilde{U}_t)^T R(x) \tilde{U}_t \right) \\ &+ \left(\mathcal{V}_t(Y_t^{(\text{opt})}) + \sum_{x \in \mathbb{S}} \pi_t(x) (U_t^{(\text{opt})} + V_t(x))^T R(x) (U_t^{(\text{opt})} + V_t(x)) \right) + (\text{cross-term}), \end{aligned}$$

where the cross-term is given by,

$$\begin{aligned} (\text{cross-term}) &= 2 \left(\pi_t(Y_t^{(\text{opt})} c^T) \tilde{U}_t - \pi_t(Y_t^{(\text{opt})}) \pi_t(c^T) \tilde{U}_t + \sum_{x \in \mathbb{S}} \pi_t(x) (U_t^{(\text{opt})} + V_t(x))^T R(x) \tilde{U}_t \right) \\ &= 2 \tilde{U}_t^T \left(\pi_t((c - \pi_t(c)) Y_t^{(\text{opt})}) + \pi_t(R) U_t^{(\text{opt})} + \pi_t(R V_t) \right) = 0. \end{aligned}$$

It remains to show that

$$\mathcal{V}_t(\tilde{Y}_t) + \sum_{x \in \mathbb{S}} \pi_t(x) (\tilde{U}_t)^T R(x) \tilde{U}_t = \langle \tilde{U}_t, \tilde{U}_t \rangle_{p_t}.$$

Because $\tilde{Y}_t(x) = c^\top(x)\tilde{U}_t$,

$$\mathcal{V}_t(\tilde{Y}_t) + \sum_{x \in \mathbb{S}} \pi_t(x) (\tilde{U}_t)^\top R(x) \tilde{U}_t = \tilde{U}_t^\top \pi_t(cc^\top) \tilde{U}_t - (\pi_t(c)^\top \tilde{U}_t)^2 + \tilde{U}_t^\top (\pi_t(R)) \tilde{U}_t.$$

From the definition of $R(x)$,

$$\begin{aligned} R(x) + c(x)c^\top(x) &= \text{diag}(c(x)) + C(x,0)(I + 11^\top), \quad x \in \mathbb{S} \\ \therefore, \quad \pi_t(R + cc^\top) &= \text{diag}(\pi_t(c)) + p_t(0)(I + 11^\top). \end{aligned}$$

Then

$$\begin{aligned} \tilde{U}_t^\top (\pi_t(R + cc^\top)) \tilde{U}_t &= \sum_{i=1}^m ((\pi_t(c))(i) + p_t(0)) (\tilde{U}_t(i))^2 + p_t(0) \left(\sum_{i=1}^m \tilde{U}_t(i) \right)^2 \\ &= \sum_{i=1}^m p_t(i) (\tilde{U}_t(i))^2 + p_t(0) \left(\sum_{i=1}^m \tilde{U}_t(i) \right)^2. \end{aligned}$$

Finally,

$$\pi_t(c)^\top \tilde{U}_t = \sum_{i=1}^m (\pi_t(c))(i) \tilde{U}_t(i) = \sum_{i=1}^m p_t(i) \tilde{U}_t(i) + p_t(0) \left(- \sum_{i=1}^m \tilde{U}_t(i) \right).$$

and the result follows.

Appendix F. Proof of Prop. 13 (Example with $m = 1$ and $T = 1$)

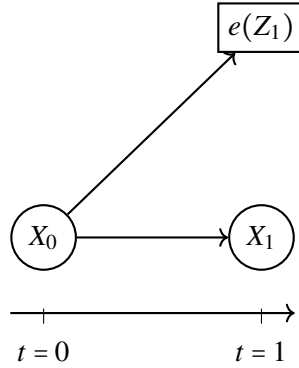


Figure 8: Graphical model for the HMM for $T = 1$.

For $T = 1$, there are only three random variables $(X_0, X_1, e(Z_1)) \in \mathbb{S} \times \mathbb{S} \times \{-1, 1\}$ whose relationship is depicted in Fig. 8. Our interest is to compute the conditional expectation $\pi_1(F) = \mathbb{E}(F(X_1) | Z_1)$ for $F \in \mathcal{Z}_1$. The formula for the same is given by,

$$\pi_1(F) = \begin{cases} \frac{\mu(c^+(AF))}{\mu(c^+)}, & \text{if } e(Z_1) = 1, \\ \frac{\mu(c^-(AF))}{\mu(c^-)}, & \text{if } e(Z_1) = -1. \end{cases} \quad (13)$$

The goal is to derive this formula from solving the OCP (3) with $T = 1$.

With $T = 1$, the OCP (3) is an example of a single-stage OCP as follows:

$$\begin{aligned} \min_{u_0 \in \mathbb{R}} \quad & \eta(u_0) := \mu(y_0^2) - \mu(y_0)^2 + \mu((u_0 + v_0)^2 r) + E((\Gamma F)(X_0)) \\ \text{subject to:} \quad & y_0(x) = (AF)(x) + c(x)(u_0 + v_0(x)) - v_0(x)e(Z_1), \quad x \in \mathbb{S}, \end{aligned}$$

where we use the lower case notation for u_0, y_0, v_0 to stress the fact that these are all deterministic (the cost $\eta(u_0) = J_1(U_0; F)$ for $U_0 = u_0$). The two random variables $F(\cdot)$ and Z_1 are denoted by capital letters. The third term in the objective, $E((\Gamma F)(X_0))$, is not affected by the choice of the decision variable u_0 .

The single-stage OCP is to choose a real number u_0 to minimize the quadratic objective, subject to a linear constraint. The only reason that the solution is not entirely elementary is because the constraint is random.

Let

$$F(x) = \begin{cases} F^+(x), & \text{if } e(Z_1) = 1, \\ F^-(x), & \text{if } e(Z_1) = -1. \end{cases}$$

Then the constraint is given by two deterministic equations

$$\begin{aligned} y_0(x) &= (AF^+)(x) + c(x)(u_0 + v_0(x)) - v_0(x), \quad x \in \mathbb{S}, \\ y_0(x) &= (AF^-)(x) + c(x)(u_0 + v_0(x)) + v_0(x), \quad x \in \mathbb{S}, \end{aligned}$$

which are readily solved to obtain formulae for the solution (y_0, v_0) as follows:

$$\begin{aligned} v_0(x) &= (A\tilde{f})(x), \quad x \in \mathbb{S}, \\ y_0(x) &= (Af)(x) + c(x)(u_0 + v_0(x)), \quad x \in \mathbb{S}, \end{aligned}$$

where $f(x) = \frac{F^+(x) + F^-(x)}{2}$ and $\tilde{f}(x) = \frac{F^+(x) - F^-(x)}{2}$. For the particular case where F is deterministic, $v_0 = 0$.

To solve the optimization problem, we consider two cases as follows:

- The case where $\mu(r) \neq 0$ (equivalently, $1 - \mu(c)^2 \neq 0$).
- The case where $\mu(r) = 0$ (equivalently, $1 - \mu(c)^2 = 0$).

• **Case where $\mu(r) \neq 0$:** Substitute the solution for y_0 into the quadratic objective, upon taking the derivative and setting it to zero, the formula for optimal control is given by,

$$u_0 = u_0^{(\text{opt})} := \frac{-1}{\mu(r)} (\mu(y_0(c - \mu(c))) + \mu(v_0 r)) = \frac{-1}{1 - \mu(c)^2} (R_1 + R_2),$$

where $R_1 = (\mu((Af)c) - \mu(Af)\mu(c))$ and $R_2 = (\mu(v_0) - \mu(v_0 c)\mu(c))$. This is the formula (5). Moreover, a completion-of-square argument gives

$$\eta(u_0) = \eta(u_0^{(\text{opt})}) + (1 - \mu(c)^2)(u_0 - u_0^{(\text{opt})})^2,$$

which shows that the optimal control is unique.

The resulting estimator is given by

$$S_1 = \mu(Af) + \mu(c(u_0 + v_0)) + \frac{R_1 + R_2}{1 - \mu(c)^2} e(Z_1)$$

$$= \begin{cases} \mu(Af) + \mu(cv_0) + \frac{1 - \mu(c)}{1 - \mu(c)^2} (R_1 + R_2), & \text{if } e(Z_1) = 1, \\ \mu(Af) + \mu(cv_0) - \frac{1 + \mu(c)}{1 - \mu(c)^2} (R_1 + R_2), & \text{if } e(Z_1) = -1. \end{cases}$$

Using the identities $\mu(c^+ - c^-) = \mu(c)$ and $\mu(c^+ + c^-) = 1$, upon simplifying,

$$\mu(Af) + \frac{R_1}{2\mu(c^+)} = \frac{\mu(c^+(Af))}{\mu(c^+)}, \quad \mu(cv_0) + \frac{R_2}{2\mu(c^+)} = \frac{\mu(c^+v_0)}{\mu(c^+)},$$

$$\mu(Af) - \frac{R_1}{2\mu(c^-)} = \frac{\mu(c^-(Af))}{\mu(c^-)}, \quad \mu(cv_0) - \frac{R_2}{2\mu(c^-)} = \frac{-\mu(c^-v_0)}{\mu(c^-)}.$$

Upon combining the terms,

$$S_1 = \begin{cases} \frac{\mu(c^+(Af+v_0))}{\mu(c^+)}, & \text{if } e(Z_1) = 1, \\ \frac{\mu(c^-(Af-v_0))}{\mu(c^-)}, & \text{if } e(Z_1) = -1. \end{cases}$$

This coincides with the formula (13) because $Af + v_0 = AF^+$ and $Af - v_0 = AF^-$. From the duality principle,

$$\eta(u_0^{\text{opt}}) = \mathbb{E}(|F(X_1) - \pi_1(F)|^2).$$

• **Case where $\mu(r) = 0$:** Set the control and the estimator as

$$u_0 = 0, \quad S_1 = \mu(y_0).$$

Because $1 - \mu(c)^2 = 4\mu(c^+)\mu(c^-)$, $1 - \mu(c)^2 = 0$ iff either $\mu(c^+) = 0$ or $\mu(c^-) = 0$. We have

$$\mu(c^+) = 0 \implies c(x) = c^+(x) - c^-(x) = -1, \quad \forall x \in \text{supp}(\mu),$$

$$\mu(c^-) = 0 \implies c(x) = c^+(x) - c^-(x) = +1, \quad \forall x \in \text{supp}(\mu).$$

Using the formula for y_0 , this gives

$$\mu(c^+) = 0 \implies S_1 = \mu(Af - v_0) = \mu(AF^-),$$

$$\mu(c^-) = 0 \implies S_1 = \mu(Af + v_0) = \mu(AF^+).$$

Because $\mu(c^\pm) = \mathbb{P}(Z_1 = \pm 1)$,

$$S_1 = \pi_1(F), \quad \text{P-a.s.}$$

Appendix G. Proof of Prop. 14

For $T = 1$, the result follows from noting that with $Y_1 = f$ (where f is deterministic) the optimal BSΔE reduces to a BDE

$$y_0 = (Af)(x) + c^T(x)\phi(y_0, 0; \mu), \quad (\because V_0 = 0).$$

From Thm. 11,

$$\pi_1(f) = \mu(y_0) - \phi(y_0, 0; \mu)^\top e(Z_1), \quad \text{P-a.s., } f \in \mathbb{R}^d$$

and therefore,

$$\pi_1^{(z_1)}(f) = \mu(y_0) - \phi(y_0, 0; \mu)^\top e(z_1), \quad f \in \mathbb{R}^d$$

Reduction to $m = 1$ is most readily seen from noting the formula for the conditional measure,

$$\pi_1^{(z_1)}(f) = \frac{\pi(C(\cdot, z_1)(Af))}{\pi(C(\cdot, z_1))}, \quad f \in \mathbb{R}^d.$$

Because the right-hand side only depends upon $C(\cdot, z_1)$, for the purpose of computing $\pi_1^{(z_1)}(f)$, we can consider the fixed-point equation for a binary-valued HMM.

For $T = 2$, repeating the argument above,

$$\pi_2^{(z_1, z_2)}(f) = \pi_1^{(z_1)}(y_1) - \phi(y_1, 0; \pi_1^{(z_1)})^\top e(z_2), \quad (\cdot, \pi_1^{(z_1)} \text{ is deterministic}),$$

and therefore,

$$\pi_2^{(z_1, z_2)}(f) = \mu(y_0) - \phi(y_0, 0; \mu)^\top e(z_1) - \phi(y_1, 0; \pi_1^{(z_1)})^\top e(z_2).$$

The general case follows by induction.

Appendix H. Pseudocodes for dual filter algorithms

Algorithm 1 Dual filter $\mathcal{N}^{(\text{dfltr})}$ (iterative)

Require: HMM parameters (A, C) , observation sequence $z = [z_1, z_2, \dots, z_T] \in \mathbb{O}^T$, measure $\rho = \{\rho_0, \rho_1, \dots, \rho_{T-1}\} \in \mathbb{R}^{d \times T}$

Ensure: Measure $\rho^+ = \{\rho_1^+, \dots, \rho_{T-1}^+, \rho_T^+\} \in \mathbb{R}^{d \times T}$

```

1:  $T \leftarrow$  length of  $z$ 
2:  $f \leftarrow I_d$  % Eq. (6c) (set f to identity matrix)
3: for  $t = T$  to 1 do
4:    $c \leftarrow 2 \cdot C(\cdot, z_t) - 1$  % Set  $c = c^+ - c^-$ 
5:    $u \leftarrow$  compute_optimal_control( $\rho_{t-1}, Af, 0, c$ ) % Eq. (6b) (Algorithm 3)
6:    $f \leftarrow Af + c \cdot u$  % Eq. (6a)
7:    $u_{t-1} \leftarrow u$ 
8:    $y_{t-1} \leftarrow f$ 
9: end for
10:  $s \leftarrow \rho_0 \cdot y_0$ 
11: for  $t = 1$  to  $T$  do
12:    $s \leftarrow s - u_{t-1}$ 
13:    $\rho_t^+ \leftarrow s \cdot y_t^\dagger$  % Eq. (6d)
14:    $\rho_t^+ \leftarrow$  normalize_distribution( $\rho_t^+$ )
15: end for
16: return  $\rho^+$ 

```

Algorithm 2 Dual filter $\mathcal{N}^{(\text{dfltr})}$ (single-shot)

Require: HMM parameters (A, C) , initial measure μ , observation sequence $z = [z_1, z_2, \dots, z_T] \in \mathbb{O}^T$

Ensure: Measure $\rho^+ = \{\rho_1^+, \rho_2^+, \dots, \rho_T^+\} \in \mathbb{R}^{d \times T}$

```

1:  $T \leftarrow$  length of  $z$ 
2: for  $t = 1$  to  $T$  do
3:    $f \leftarrow I_d$                                      % Eq. (6c) (set f to identity matrix)
4:    $s \leftarrow 0$ 
5:   for  $\tau = t$  to 1 do
6:      $c \leftarrow 2 \cdot C(:, z_\tau) - 1$                  % Set  $c = c^+ - c^-$ 
7:      $u \leftarrow$  compute_optimal_control( $\rho_{\tau-1}^+, Af, 0, c$ ) % Eq. (6b) (Algorithm 3)
8:      $f \leftarrow Af + c \cdot u$                          % Eq. (6a)
9:      $s \leftarrow s - u$ 
10:  end for
11:   $s \leftarrow s + \mu \cdot f$ 
12:   $\rho_t^+ \leftarrow$  normalize_distribution( $s$ )
13: end for
14: return  $\rho^+$ 

```

Algorithm 3 Computation of control input u

Require: Measure ρ , functions g, v , and c (all are elements of \mathbb{R}^d)

Ensure: Control $u \in \mathbb{R}$

```

1: if  $\rho(c)^2 = 1$  then
2:    $u \leftarrow 0$ 
3: else
4:    $u \leftarrow -\frac{1}{1-\rho(c)^2} \cdot ((\rho(g \cdot c) - \rho(g)\rho(c)) + (\rho(v) - \rho(v \cdot c)\rho(c)))$ 
5: end if
6: return  $u$ 

```

Algorithm 4 Initialization of ρ

Require: HMM parameters (μ, C) , obs. sequence $z = [z_1, z_2, \dots, z_T]$

Ensure: Measure $\rho = \{\mu, \rho_1, \dots, \rho_{T-1}, \rho_T\}$

```

1:  $\rho_0 \leftarrow \mu$ 
2: for  $t = 1$  to  $T$  do
3:    $\rho_t \leftarrow C(:, z_t)$ 
4:    $\rho_t \leftarrow$  normalize_distribution( $\rho_t$ )
5: end for
6: return  $\rho$ 

```

Algorithm 5 Projection and normalization of measure

Require: Signed measure σ

Ensure: Probability measure ρ

```

1:  $\rho \leftarrow \max(\sigma, 0)$                                      % clip negative values to 0
2:  $\rho \leftarrow \rho / \text{sum}(\rho)$                              % normalize
3: return  $\rho$ 

```

Algorithm 6 Nonlinear prediction p

Require: HMM parameters C , measure $\rho = \{\rho_0, \rho_1, \dots, \rho_{T-1}, \rho_T\} \in \mathbb{R}^{d \times (T+1)}$

Ensure: Measure $p = \{p_1, \dots, p_T\} \in \mathbb{R}^{m \times T}$

- 1: **for** $t = 1$ to T **do**
 - 2: $p_t \leftarrow \rho_t \cdot C$
 - 3: **end for**
 - 4: **return** p
-

Algorithm 7 Sampling a random matrix

Require: row dim d , column dim m , temperature τ

Ensure: Random matrix $M \in \mathbb{R}^{d \times m}$

- 1: **for** $i = 1$ to d **do**
 - 2: $M(i, :) \leftarrow \text{softmax}(\text{randn}(m)/\tau)$
 - 3: **end for**
 - 4: **return** M
-

Appendix I. Additional operations in a transformer

This section is based on (Jurafsky and Martin, 2025, Ch., 10). Fix t . The output y_t from concatenating the output of multiple heads is subject to the following operations:

1. Residual connection which means

$$y_t \mapsto y_t + e_t.$$

2. Layer normalization which means

$$y_t \mapsto \text{diag}(\gamma) \frac{y_t - \text{mean}(y_t)}{\text{std}(y_t)} + \beta.$$

where $\gamma \in \mathbb{R}^d$ and $\beta \in \mathbb{R}^d$ are learnable parameters (referred to as gain and offset).

3. Feedforward neural network

$$y_t \mapsto \text{FFN}(y_t).$$

I.1 Summary of operations in a single layer

Fix time t . The following operations define a single layer in a transformer:

$$y_t = \text{MultiHeadAttention}(e_t, [e_1, e_2, \dots, e_{t-1}])$$

$$y_t = y_t + e_t$$

$$y_t = \text{LayerNorm}(y_t)$$

$$y_t = y_t + \text{FFN}(y_t)$$

$$y_t = \text{LayerNorm}(y_t)$$

The learnable parameters in the MultiHeadAttention are the matrices W_V, W_K, W_Q, W_O . For each of the two LayerNorm operations, the learnable parameters are the gains γ and the offset β . Additionally, the weights of the FFN are also learned.

Parameter	Transformer	Dual filter	Training Parameter	nanoGPT
Context length	$T = 256$	256	Learning rate	10^{-3}
Vocabulary size	$m = 65$	65	Minimum learning rate	10^{-4}
State (embedding) dim	$d = 384$	384	Learning rate decay	cosine
Number of layers	$L = 6$	6	Learning rate decay steps	2000
Number of heads	$n_{\text{head}} = 6$	N/A	Optimizer	AdamW
FFN dimension	1536	N/A	Batch size	10
Output temperature	1	N/A	Dropout	0.1

Table 6: Summary of model parameters for the numerical experiments. The left table lists the architectural parameters, while the right table lists the training parameters specific to the nanoGPT transformer.

Appendix J. Numerical Experiments with Transformer

The numerical experiments described in Sec. 5 were repeated using a nanoGPT transformer (Karpathy, 2024). The observations are generated from an HMM. The HMM parameters are the same as described in Sec. 5, specifically, $d = 384$, $m = 65$, and $T = 256$, and other parameters are as follows:

- The prior μ is set to the uniform probability vector: $\mu(x) = \frac{1}{d}$ for $x \in \mathbb{S}$.
- The transition matrix $A = A^{(\text{circ})}$.
- The emission matrix C is randomly sampled. See Algorithm 7 for details.

For this model, the numerical results using the dual filter are given in Fig. 4 and Fig. 5.

As a first step, the nanoGPT is trained using the observation data sampled from the HMM(μ, A, C). The nanoGPT hyper-parameters were carefully tuned to ensure optimal performance (see Table 6). Note that the dual filter theory is entirely model-based. So, there is no training step to obtain the numerical results reported in Sec. 5.

As a second step, the trained nanoGPT model is used for inference and its prediction performance numerically evaluated. For this purpose, the observations $z = \{z_1, z_2, \dots, z_T\}$ are generated from the same HMM(μ, A, C) used for training. The inference results were mixed, depending upon the randomly sampled C . There are two cases as follows:

- **Favorable case.** See left panel of Fig. 9. Here, nanoGPT produces predictions p_t that are good approximations of the ground truth computed from the model-based nonlinear filter. Quantitatively, the error $\varepsilon_t^{(\ell)}$ starts near 1 at the first layer and progressively decays with each subsequent layer, reaching values in the range 10^{-1} to 10^{-4} at the final layer ($\ell = L$). The top-ten conditional probabilities closely match the ground truth for all time points, indicating successful learning and inference.
- **Unfavorable case.** See right panel of Fig. 9. Here, the nanoGPT predictions are not accurate. The error $\varepsilon_t^{(\ell)}$ remains high throughout all layers and does not exhibit the progressive decay seen in the favorable case. The top-ten conditional probabilities deviate substantially from the ground truth, reflecting a failure to learn an accurate predictive distribution.

Notably, the results described in Fig. 4 and Fig. 5 are for the unfavorable case.

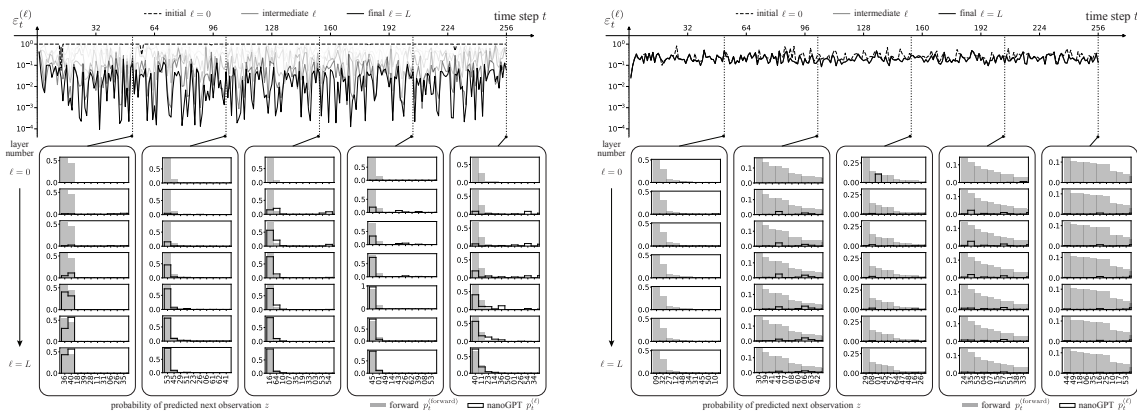


Figure 9: Comparison of transformer predictions against the ground truth from the nonlinear filter, for two choices of the randomly sampled emission matrix C . **(Left)** Favorable case: the error decays from near 1 to the range 10^{-1} – 10^{-4} by the final layer, and the predicted conditional probability closely matches the ground truth. **(Right)** Unfavorable case (same HMM instance as Fig. 5): the error remains high across all layers and the predicted conditional probability does not converge to the ground truth. Each panel shows: (Top) time traces of the per-step error $\{\varepsilon_t^{(\ell)} : 1 \leq t \leq T\}$ for layers $\ell = 1, 2, \dots, L$ (with $L = 6$); the dashed line is the error immediately after embedding ($\ell = 0$), and solid lines show subsequent layers with darker shades used as ℓ increases. (Bottom) top-ten conditional probabilities $\{p_t^{(\ell)}(z_i)\}$ at five representative time points, sorted in decreasing order; the gray shading is the ground truth and the solid line is the transformer output.

The numerical results suggest that while the transformer can learn to approximate the nonlinear filter in some cases, its performance is sensitive to the choice of the emission matrix C . An empirical observation is that in the favorable case, the conditional probability p_t is supported on a relatively small subset of the vocabulary \mathbb{O} — suggesting that the transformer performs well when the prediction task is, in some sense, low-complexity. Without a suitable theoretical framework, it is difficult to make this precise.

References

Álvaro Rodríguez Abella, João Pedro Silvestre, and Paulo Tabuada. The asymptotic behavior of attention in transformers. *arXiv preprint arXiv:2412.02682*, 2024.

Daniel Owusu Adu and Bahman Ghahsifard. Approximate controllability of continuity equation of transformers. *IEEE Control Systems Letters*, 2024.

Ahmed M Alaa and Mihaela van der Schaar. Attentive state-space modeling of disease progression. *Advances in neural information processing systems*, 32, 2019.

Elie Azeraf, Emmanuel Monfrini, Emmanuel Vignon, and Wojciech Pieczynski. Introducing the hidden neural Markov chain framework. *arXiv preprint arXiv:2102.11038*, 2021.

David Barber, A Taylan Cemgil, and Silvia Chiappa. Inference and estimation in probabilistic time series models. *Bayesian Time Series Models*, 1, 2011.

- A. Bensoussan. *Estimation and Control of Dynamical Systems*, volume 48. Springer, 2018.
- Aman Bhargava, Cameron Witkowski, Shi-Zhuo Looi, and Matt Thomson. What’s the magic word? a control theory of llm prompting. *arXiv preprint arXiv:2310.04444*, 2023.
- Joan Bruna and Daniel Hsu. Survey on algorithms for multi-index models. *arXiv preprint arXiv:2504.05426*, 2025.
- Frank M Callier and Charles A Desoer. *Linear system theory*. Springer Science & Business Media, 2012.
- Olivier Cappé, Eric Moulines, and Tobias Rydén. *Inference in hidden Markov models*. Springer Science & Business Media, 2006.
- Valérie Castin, Pierre Ablin, José Antonio Carrillo, and Gabriel Peyré. A unified perspective on the dynamics of deep transformers. *arXiv preprint arXiv:2501.18322*, 2025.
- Lili Chen, Kevin Lu, Aravind Rajeswaran, Kimin Lee, Aditya Grover, Misha Laskin, Pieter Abbeel, Aravind Srinivas, and Igor Mordatch. Decision transformer: Reinforcement learning via sequence modeling. *Advances in neural information processing systems*, 34:15084–15097, 2021.
- Reginald Zhiyan Chen, Heng-Sheng Chang, and Prashant G Mehta. Belief net: A filter-based framework for learning hidden markov models from observations. In *8th Annual Learning for Dynamics and Control Conference*. PMLR, 2026.
- Ta-Chung Chi, Ting-Han Fan, Peter J Ramadge, and Alexander Rudnicky. Kerple: Kernelized relative positional embedding for length extrapolation. *Advances in Neural Information Processing Systems*, 35:8386–8399, 2022.
- P Chigansky, R Liptser, and R Van Handel. Intrinsic methods in filter stability. In Dan Crisan and Boris Rozovskii, editors, *Handbook of Nonlinear Filtering*. Oxford University Press, 2009.
- Samuel N Cohen and Robert J Elliott. A general theory of finite state backward stochastic difference equations. *Stochastic Processes and their Applications*, 120(4):442–466, 2010.
- Zihang Dai, Zhilin Yang, Yiming Yang, Jaime Carbonell, Quoc V Le, and Ruslan Salakhutdinov. Transformer-xl: Attentive language models beyond a fixed-length context. *arXiv preprint arXiv:1901.02860*, 2019.
- Robert J Elliott, Lakhdar Aggoun, and John B Moore. *Hidden Markov models: estimation and control*, volume 29. Springer Science & Business Media, 2008.
- Masaaki Fukasawa, Takashi Sato, and Jun Sekine. Backward stochastic difference equations on lattices with application to market equilibrium analysis. *Journal of Applied Probability*, pages 1–27, 2025.
- Borjan Geshkovski, Cyril Letrouit, Yury Polyanskiy, and Philippe Rigollet. A mathematical perspective on transformers. *arXiv preprint arXiv:2312.10794*, 2023.
- Borjan Geshkovski, Philippe Rigollet, and Domènec Ruiz-Balet. Measure-to-measure interpolation using transformers. *arXiv preprint arXiv:2411.04551*, 2024.

- Gautam Goel and Peter Bartlett. Can a transformer represent a kalman filter? In *6th Annual Learning for Dynamics & Control Conference*, pages 1502–1512. PMLR, 2024.
- Alex Graves. Generating sequences with recurrent neural networks. *arXiv preprint arXiv:1308.0850*, 2013.
- Xingang Guo, Darioush Keivan, Usman Syed, Lianhui Qin, Huan Zhang, Geir Dullerud, Peter Seiler, and Bin Hu. Controlagent: Automating control system design via novel integration of llm agents and domain expertise. *arXiv preprint arXiv:2410.19811*, 2024.
- Chi Han, Ziqi Wang, Han Zhao, and Heng Ji. Explaining emergent in-context learning as kernel regression. *arXiv preprint arXiv:2305.12766*, 2023.
- Hangfeng He and Weijie J Su. A law of next-token prediction in large language models. *arXiv preprint arXiv:2408.13442*, 2024.
- Omar Bakri Hijab. *Minimum Energy Estimation*. PhD thesis, University of California, Berkeley, 1980.
- M Emrullah Ildiz, Yixiao Huang, Yingcong Li, Ankit Singh Rawat, and Samet Oymak. From self-attention to markov models: Unveiling the dynamics of generative transformers. *arXiv preprint arXiv:2402.13512*, 2024.
- Herbert Jaeger. Observable operator models for discrete stochastic time series. *Neural computation*, 12(6):1371–1398, 2000.
- Michael I Jordan, Zoubin Ghahramani, Tommi S Jaakkola, and Lawrence K Saul. An introduction to variational methods for graphical models. *Machine learning*, 37:183–233, 1999.
- Daniel Jurafsky and James H. Martin. *Speech and Language Processing: An Introduction to Natural Language Processing, Computational Linguistics, and Speech Recognition with Language Models*. 3rd edition, 2025. URL <https://web.stanford.edu/~jurafsky/slp3/>. Online manuscript released January 12, 2025.
- Thomas Kailath, Ali H Sayed, and Babak Hassibi. *Linear Estimation*. Prentice Hall, 2000.
- Hsu Kao and Vijay Subramanian. Common information based approximate state representations in multi-agent reinforcement learning. In *International Conference on Artificial Intelligence and Statistics*, pages 6947–6967. PMLR, 2022.
- Andrej Karpathy. Nanogpt. <https://github.com/karpathy/nanoGPT>, 2022. Commit 325be85d9be8c81b436728a420e85796c57dba7e.
- Andrej Karpathy. nanogpt: The simplest, fastest repository for training/finetuning medium-sized gpts. <https://github.com/karpathy/nanoGPT>, 2024.
- Jin Won Kim and Prashant G. Mehta. An optimal control derivation of nonlinear smoothing equations. In *Proceedings of the Workshop on Dynamics, Optimization and Computation held in honor of the 60th birthday of Michael Dellnitz*, pages 295–311. Springer, 2020.

- Jin Won Kim and Prashant G. Mehta. Duality for nonlinear filtering I: Observability. *IEEE Transactions on Automatic Control*, 69(2):699–711, 2024a. doi: 10.1109/TAC.2023.3279206.
- Jin Won Kim and Prashant G. Mehta. Duality for nonlinear filtering II: Optimal control. *IEEE Transactions on Automatic Control*, 69(2):712–725, 2024b. doi: 10.1109/TAC.2023.3279208.
- Jin Won Kim and Prashant G. Mehta. Variance decay property for filter stability. *IEEE Transactions on Automatic Control*, 69(12):8140–8155, 2024c. doi: 10.1109/TAC.2024.3413573.
- Jin Won Kim and Prashant G Mehta. The arrow of time in estimation and control: Duality theory beyond the linear Gaussian model. *IEEE Control Systems Magazine*, 45(2):70–90, 2025.
- Jin Won Kim, Prashant G. Mehta, and Sean Meyn. What is the Lagrangian for nonlinear filtering? In *2019 IEEE 58th Conference on Decision and Control (CDC)*, pages 1607–1614, Nice, France, 12 2019a. IEEE.
- Jin Won Kim, Amirhossein Taghvaei, Prashant G. Mehta, and Sean Meyn. An approach to duality in nonlinear filtering. In *2019 American Control Conference (ACC)*, pages 5360–5365, Philadelphia, PA, 2019b.
- Jin Won Kim, Anant A. Joshi, and Prashant G. Mehta. Backward map for filter stability analysis. In *2024 IEEE 63rd Conference on Decision and Control (CDC)*, pages 4070–4077, 2024. doi: 10.1109/CDC56724.2024.10886772.
- Daphne Koller and Nir Friedman. *Probabilistic Graphical Models: Principles and Techniques*. MIT Press, 2009.
- Lingkai Kong, Haorui Wang, Wenhao Mu, Yuanqi Du, Yuchen Zhuang, Yifei Zhou, Yue Song, Rongzhi Zhang, Kai Wang, and Chao Zhang. Aligning large language models with representation editing: A control perspective. *Advances in Neural Information Processing Systems*, 37:37356–37384, 2024.
- Michael Littman and Richard S Sutton. Predictive representations of state. *Advances in neural information processing systems*, 14, 2001.
- Bingbin Liu, Daniel J Hsu, Pradeep Ravikumar, and Andrej Risteski. Masked prediction: A parameter identifiability view. *Advances in Neural Information Processing Systems*, 35:21241–21254, 2022.
- Tian Yu Liu, Stefano Soatto, Matteo Marchi, Pratik Chaudhari, and Paulo Tabuada. Observability of latent states in generative ai models.
- Yifan Luo, Yiming Tang, Chengfeng Shen, Zhennan Zhou, and Bin Dong. Prompt engineering through the lens of optimal control. *arXiv preprint arXiv:2310.14201*, 2023.
- Andrew Kachites McCallum. *Reinforcement learning with selective perception and hidden state*. University of Rochester, 1996.
- Kevin McGoff, Sayan Mukherjee, and Natesh Pillai. Statistical inference for dynamical systems: A review. 2015.

- S. K. Mitter and N. J. Newton. A variational approach to nonlinear estimation. *SIAM Journal on Control and Optimization*, 42(5):1813–1833, 2003.
- R. E. Mortensen. Maximum-likelihood recursive nonlinear filtering. *Journal of Optimization Theory and Applications*, 2(6):386–394, 1968.
- Mary Phuong and Marcus Hutter. Formal algorithms for transformers. *arXiv preprint arXiv:2207.09238*, 2022.
- Ofir Press, Noah A Smith, and Mike Lewis. Train short, test long: Attention with linear biases enables input length extrapolation. *arXiv preprint arXiv:2108.12409*, 2021.
- Maxim Raginsky. A variational approach to sampling in diffusion processes. In *2024 IEEE 63rd Conference on Decision and Control (CDC)*, Dec 2024.
- Sebastian Raschka. *Build a Large Language Model (From Scratch)*. Simon and Schuster, 2024.
- Hongyu Ren, Hanjun Dai, Zihang Dai, Mengjiao Yang, Jure Leskovec, Dale Schuurmans, and Bo Dai. Combiner: Full attention transformer with sparse computation cost. *Advances in Neural Information Processing Systems*, 34:22470–22482, 2021.
- Raanan Y Rohekar, Yaniv Gurwicz, and Shami Nisimov. Causal interpretation of self-attention in pre-trained transformers. *Advances in Neural Information Processing Systems*, 36:31450–31465, 2023.
- Matthew Rudary and Satinder Singh. A nonlinear predictive state representation. *Advances in neural information processing systems*, 16, 2003.
- Michael E Sander, Pierre Ablin, Mathieu Blondel, and Gabriel Peyré. Sinkformers: Transformers with doubly stochastic attention. In *International Conference on Artificial Intelligence and Statistics*, pages 3515–3530. PMLR, 2022.
- Stefano Soatto, Paulo Tabuada, Pratik Chaudhari, and Tian Yu Liu. Taming ai bots: Controllability of neural states in large language models. *arXiv preprint arXiv:2305.18449*, 2023.
- Jayakumar Subramanian, Amit Sinha, Raihan Seraj, and Aditya Mahajan. Approximate information state for approximate planning and reinforcement learning in partially observed systems. *Journal of Machine Learning Research*, 23(12):1–83, 2022.
- Tobias Sutter, Arnab Ganguly, and Heinz Koepl. A variational approach to path estimation and parameter inference of hidden diffusion processes. *Journal of Machine Learning Research*, 17(190):1–37, 2016. URL <http://jmlr.org/papers/v17/16-075.html>.
- Binh Tang and David S Matteson. Probabilistic transformer for time series analysis. *Advances in Neural Information Processing Systems*, 34:23592–23608, 2021.
- Emanuel Todorov. General duality between optimal control and estimation. In *2008 IEEE 47th Conference on Decision and Control (CDC)*, pages 4286–4292, 12 2008.
- Ramon van Handel. *Filtering, stability, and robustness*. PhD thesis, California Institute of Technology, Pasadena, 12 2006.

- Ramon van Handel. Observability and nonlinear filtering. *Probability Theory and Related Fields*, 145(1-2):35–74, 2009.
- Ashish Vaswani, Noam Shazeer, Niki Parmar, Jakob Uszkoreit, Llion Jones, Aidan N Gomez, Lukasz Kaiser, and Illia Polosukhin. Attention is all you need. *Advances in neural information processing systems*, 30, 2017.
- James Vuckovic, Aristide Baratin, and Remi Tachet des Combes. A mathematical theory of attention. *arXiv preprint arXiv:2007.02876*, 2020.
- Martin J. Wainwright and Michael I. Jordan. *Graphical Models, Exponential Families, and Variational Inference*, volume 1 of *Foundations and Trends in Machine Learning*. Now Publishers Inc., 2008. doi: 10.1561/22000000001.
- Weiyue Wang, Derui Zhu, Tamer Alkhouli, Zixuan Gan, and Hermann Ney. Neural hidden Markov model for machine translation. In Iryna Gurevych and Yusuke Miyao, editors, *Proceedings of the 56th Annual Meeting of the Association for Computational Linguistics (Volume 2: Short Papers)*, pages 377–382, Melbourne, Australia, July 2018. Association for Computational Linguistics. doi: 10.18653/v1/P18-2060. URL <https://aclanthology.org/P18-2060/>.
- Weiyue Wang, Zijian Yang, Yingbo Gao, and Hermann Ney. Transformer-based direct hidden Markov model for machine translation. In *Proceedings of the 59th Annual Meeting of the Association for Computational Linguistics and the 11th International Joint Conference on Natural Language Processing: Student Research Workshop*, pages 23–32, 2021.
- Stephen Wolfram. *What Is ChatGPT Doing... and Why Does It Work?* Wolfram Media, 2023.
- Sang Michael Xie, Aditi Raghunathan, Percy Liang, and Tengyu Ma. An explanation of in-context learning as implicit Bayesian inference. *arXiv preprint arXiv:2111.02080*, 2021.
- Jie Xiong. *An Introduction to Stochastic Filtering Theory*, volume 18. Oxford University Press on Demand, 2008.
- Serdar Yüksel. Another look at partially observed optimal stochastic control: Existence, ergodicity, and approximations without belief-reduction. *Applied Mathematics & Optimization*, 91(1):16, 2025.
- Chulhee Yun, Srinadh Bhojanapalli, Ankit Singh Rawat, Sashank J Reddi, and Sanjiv Kumar. Are transformers universal approximators of sequence-to-sequence functions? *arXiv preprint arXiv:1912.10077*, 2019.
- Shaolei Zhang and Yang Feng. Hidden markov transformer for simultaneous machine translation. In *International Conference on Learning Representations (ICLR)*, 2023. URL <https://openreview.net/forum?id=9y0HFvaAYD6>.
- Xiangyuan Zhang, Weichao Mao, Haoran Qiu, and Tamer Başar. Decision transformer as a foundation model for partially observable continuous control. *arXiv preprint arXiv:2404.02407*, 2024.
- Ingvar Ziemann, Nikolai Matni, and George J Pappas. State space models, emergence, and ergodicity: How many parameters are needed for stable predictions? *arXiv preprint arXiv:2409.13421*, 2024.